REPORT DOCUMENTATION PAGE

Form Approved
OMB No. 0704-0188

1. AGENCY USE ONLY (Leave blank)	2. REPORT DATE	3. REPORT TYPE AND DATES COVERED
	December 15, 2003	Final 02/01/99 to 9/30/03

4. TITLE AND SUBTITLE
The Near-wall Behavior of Unsteady Vortical Flow Around the Tip of an Axial Pump Rotor Blade

5. FUNDING NUMBERS
N00014-99-1-0302

6. AUTHORS
Roger L. Simpson

7. PERFORMING ORGANIZATION NAME(S) AND ADDRESS(ES)
Department of Aerospace and Ocean Engineering
Virginia Polytechnic Institute and State University
Blacksburg, Virginia 24061-0203

8. PERFORMING ORGANIZATION REPORT NUMBER

9. SPONSORING/MONITORING AGENCY NAME(S) AND ADDRESS(ES)
Office of Naval Research, 800 N. Quincy Street
Arlington, Virginia 22217

10. SPONSORING/MONITORING AGENCY REPORT NUMBER

11. SUPPLEMENTARY NOTES

12a. DISTRIBUTION/AVAILABILITY STATEMENT
Unlimited

12b. DISTRIBUTION CODE

13. ABSTRACT (Maximum 200 words)   Experimental study of three-dimensional turbulent tip gap flows in the linear cascade wind tunnel for two different tip gap clearances (t/c=1.65% and 3.3%). Three experimental techniques are used to measure the tip gap velocity field and static pressure field on the end-wall: a three-orthogonal-velocity-component fiber-optic laser Doppler anemometer (3D-LDA) system, surface oil flow visualization, and a scani-valve pressure measurement system. The end-wall skin friction velocity is calculated from near-wall LDA data and pressure gradient data using the near-wall momentum equation.

The statistics of Reynolds stresses and triple products in the two-dimensional turbulent boundary layer and three-dimensional turbulent boundary layer were examined using a velocity fluctuation octant analysis. For the three-dimensional turbulent boundary layer in the moving wall flow, the near-wall shear flow reinforces the sweep motion to the moving wall and weakens the out-ward ejection motion in the shear flow dominant region. Between the passage flow and the shear flow is the interaction region of the high speed streaks and the low speed streaks. This is the first time that the coherent structure of the three-dimensional turbulent boundary in the linear cascade tip gap has been studied.

Experimental study of the downstream behavior of vortex generators used to simulate stator trailing vortices was also done as part of this program and was described in an earlier Technical Report.

14. SUBJECT TERMS Three-dimensional Flow, Turbulent Boundary Layers, compressor flows, tip gap flows

15. NUMBER OF PAGES
36

16. PRICE CODE

17. SECURITY CLASSIFICATION OF REPORT	18. SECURITY CLASSIFICATION OF THIS PAGE	19. SECURITY CLASSIFICATION OF ABSTRACT	20. LIMITATION OF ABSTRACT
UNCLASSIFIED	UNCLASSIFIED	UNCLASSIFIED	UNLIMITED

20040317 122

Final Contract Report, 02/01/99 through 09/30/03

Contract Number	N00014-99-1-0302
Title of Research	The near-wall behavior of unsteady vortical flow around the tip of an axial pump rotor blade
Principal Investigator	Roger L. Simpson
Organization	Virginia Polytechnic Institute and State University Department of Aerospace and Ocean Engineering Blacksburg, VA 24061-0203

Technical Section

Technical Objectives

The long term objective of this research is to understand fully and quantitatively document the near-wall turbulent flow phenomena that occur downstream of an axial pump strut flow, in and around the rotor-blade tip gap, and downstream of the rotor, with the view to prediction and eventual elimination of the associated intermittent cavitation. Immediate objectives are to replicate the flow phenomena observed upstream and downstream of the rotor blade tips in an idealized laboratory environment where detailed measurements are possible and to document the structure of this flow by providing boundary conditions for LES computations and results for comparison with LES computations that reveal the physics responsible for the cavitation. These measurements will provide the first detailed quantitative view of what happens to the turbulence when an organized vortical wake encounters the tip gap between a blade tip and endwall in relative motion. These data are key to resolving the cavitation problem. They will provide crucial work for LES calculations and accompanying hot-wire anemometer studies.

The tip gap region of a turbo-machine rotor is particularly important. All of the vorticity within a flowfield is generated at walls under the action of pressure gradients and moving wall shear. This non-isotropic non-equilibrium 3-D tip gap flow generates the shed tip vortex structures that produce cavitation and noise downstream. Thus, the ___sources___ of the vorticity that enter the blade wake are in the tip gap region and are the focus of this research program. Knowledge of these sources may lead to their control to eliminate "sub-visual" cavitation.

In the current program we are obtaining fine-spatial-resolution (50 micron or $y^+ \approx$ 3) turbulence structural data within and around the tip gap of an axial pump rotor blade for several gap to chord spacings and using a stationary or moving end wall, which simulates an actual turbomachine. Detailed Reynolds stress tensor and complete triple product turbulence diffusion data are being obtained inside of the tip gap ___for the first time.___ (This is not an exaggeration since no one else has had a 3-velocity-component laser-Doppler velocimeter system with fine spatial resolution.) Measurements very close to the wall (50 microns) have been made, which permits the direct determination of wall shearing stresses in a gap flow ___for the first time without assumptions___. The detailed Reynolds stress and turbulent diffusion data are the first available to modify turbulence models for the tip gap region. These data are part of comprehensive test case data sets,

which include wake hot-wire data from Devenport's group, that will be used for comparisons with calculations.

Technical Approach

In conjunction with a related project (Devenport, 1999) experiments are being performed in the Virginia Tech Fan Cascade Wind Tunnel. This facility contains a 7-passage linear cascade with 8 GE rotor B compressor blades. The endwall beneath the blade row includes a 27"-wide Mylar belt that can be propelled by means of a roller system at up to 25m/s to simulate the relative motion of the blade tips and casing. This facility can accommodate the addition of vortex generators to the belt upstream of the blade row. These vortex generators simulate the influence of the upstream struts on the axial pump rotor flow. All components of mean velocities, turbulent stresses, triple products, and skin friction are being made with a special miniature custom-designed 3-velocity-component fiber-optic LDV that views the flow through the Mylar belt in a 30 μm diameter measurement volume within 50μm of the wall or below $y^+ = 5$ in these flows. An optical system has been developed (Devenport, 1999) to sense the instantaneous vortex generator spanwise position so that the LDV data can be sorted by vortex generator position. Another optical system (BELT-HITE) for sensing the Mylar belt vertical location within a few microns uncertainty has also been developed during this project in order to permit sorting of the LDV data with respect to the relative probe volume distance from the belt. LDV data are being obtained along the moving belt and around the sides of the tip of the blade. The quantities sought are mean velocities, Reynolds shear stresses and triple products, circulation, vorticity, TKE, turbulence diffusion rates, eddy viscosities, contributions from sweeps and ejections and wall shear stresses.

Progress

Progress During the First 3 Years, 2/1/99 to 2/28/02

The previous work on this project during these 3 years makes the current and future work possible. The Annual Progress Report for this Grant that was submitted during August 2001 gave more detail of this progress during the first 3 years. During the first year (99-00), the 3D-LDV was modified and used in an auxiliary boundary layer facility (1) to examine the behavior of a number of possible boundary layer trips for the cascade facility flows and (2) to completely document the behavior of pairs of vortex generators that are used to simulate upstream struts in the cascade flow. At the same time, a BELT-HITE system was developed to measure the moving belt vertical motion within 1 micron.

During the second year (00-01), a number of hardware modifications to the cascade wind tunnel were made to accommodate the LDV measurements next to a moving wall. An LDV signal processing system dedicated to the cascade tunnel was acquired from AOE internal resources. A number of computer hardware and software problems were solved that permitted simultaneous acquisition of 3 components of LDV signal, the moving belt height, and the upstream moving vortex generator position. Preliminary measurements of the blade inflow were made.

During the third year (01–02), measurements were obtained (1) upstream and inside the tip gap for x/c < 0.25 for the 3.3% thickness to chord case with no moving wall (Figure 1a), (2) one complete velocity profile with the moving wall and no vortex generators upstream of the blade, and (3) data downstream of the vortex generator that characterize the wake of the vortices and provide an estimate of the circulation strength of the vortices. These data were reported in the MS thesis by D. D. Kuhl (Kuhl and Simpson, 2001).

LDV optical table equipment that was borrowed from NSWCCD was returned in June 2001, at the same time that we had to vacate the Low-Speed Cascade Tunnel facility to allow Devenport's group to obtain hot-wire data. Beginning in June 2001 we have assembled new LDV optical table equipment (with ONR support) and have worked on the improvements to the Cascade facility for our LDV measurements. ONR provided 15% of the funds for a new Argon-ion laser, so now we have sufficient laser power to obtain a higher data rate. The LDV system was reconstructed. It should be noted that during the first 2 ½ years, more than 5 man-years of research effort were devoted to this program, even though ONR only supported about 3 man-years.

As a result of this experience, further hardware improvement were needed. Since June 2001, we have also identified and developed concrete plans to improve the data rate and productivity of the cascade facility for: (1) reducing the scratching of the moving belt where LDV measurements are required by eliminating the lateral meandering of the belt, (2) eliminating Teflon belt particles that obscure the LDV vision, and (3) increasing the belt life, all at a cost of $4000. The use of an automatic belt tracking system will not only eliminate the scratching of the belt over the zone of measurements, but also eliminate the current need for a second person to be continually adjusting the belt roller.

Progress During the 4th Year, 3/1/02 to 2/28/03

During the last part of the third year (11/01/01 - 2/28/02), we planned to obtain LDV data for the stationary wall case within the tip gap for (1) 3.3% tip gap to chord over the remainder of the x/c range, x/c > 0.75 and (2) 1.65% tip gap to chord over the entire 0 < x/c < 1 range. These 2 cases complement the hot-wire wake data of Devenport's group for the non-moving wall cases and provide the information on the sources of the vorticity in the flow. We expected to get access to the cascade tunnel from Devenport about 1/1/02, but did not get access until late February 2002.

However, since then we obtained the most thorough sets of LDV data in the tip gap that have been obtained to date. No other known investigation has used such a fine resolution 3-velocity-component LDV to obtain all mean velocities, Reynolds stresses, and triple products. For each of these 2 tip gaps, data at chordwise locations of x/c = 0.04, 0.09, 0.12, 0.18, 0.27, 0.42, 0.65, and 1.00 show the development of the tip gap vortex and the associated separated flow on the end wall and the reattachment on the suction side of the blade tip. After studying these data, we obtained more data around the separations. Multiple velocity profiles very close to the end wall have provided skin friction values. Well over 100 velocity profiles were obtained, each requiring setup and apparatus adjustment time to ensure the exact measurement positions and a high LDV data rate.

Figure 1b shows the co-ordinate systems that are used to present these data. The "bed system" is the same as in Figure 1a. The "chord system" is aligned with the chord of

the blade. The flow under the blade through the tip gap is almost in a direction perpendicular to the chord for the last half or so of the chord length, so this co-ordinate system allows one the see the crossflow better.

Figures 2 and 3 show in color the LDV data for the mean velocity vectors of the U (x direction) and W (z direction) components under and around the tip gap for the tip gap of 1.65% of the chord length. The beginning of each arrow is located at the (x,z) position where the measurements were made. The length of the arrow is proportional to the mean velocity magnitude. For these data in and around the gap, the arrow length is short near the end wall and is progressively in a direction nearly perpendicular to the chord as the flow moves downstream. The longer arrows are in the middle of the gap and the short arrows that are about in the chordwise direction are within the flow near the blade end. Also shown on these figures in black are the hot-wire anemometer data of Devenport's group for locations away from the wall. These results are in general qualitative agreement with the LDV data. Figure 3 shows the data that are available between 2 adjacent blades. Figure 4 shows the combined LDV and hot-wire data V-W vectors in the bed co-ordinate system for 2 planes. The LDV data in color show the near-wall boundary layer behavior.

Figures 5 is the same data as for Figure 2, except that the hot-wire anemometer data are not shown. Figure 6 shows the same data and shows the U-V mean velocity crossflows within the tip gap in the bed co-ordinate system. Figure 7 is more informative and shows the V-W crossflows in the chord co-ordinate system. The rectangular box shown at each data plane represents the blade at that location. The flow is pushed into the gap by the pressure difference between the pressure and suction sides of the blade, so we see that V is negative on the pressure (right) side of the blade, goes to zero under the blade and becomes positive on the suction side. The W magnitude strongly increases from the pressure to suction sides of the blade. As one proceeds downstream, the maximum W magnitude increases until $x/c = 0.42$ and then decreases. Figures 8 and 9 show similar features for the 3.3% tip gap to chord ratio case.

Because the origin of the vorticity in the non-moving wall cases is from the pressure gradients on the walls, complete end wall surface pressure measurements were made under the tip gap over a large area using a small spacing between pressure taps. This allows us to determine the vector pressure gradient on the wall.

Oilflow surface skin-friction visualizations have also been made to determine the locations of the tip vortex induced separation on the end wall and the reattachment on the end of the blade.

Two graduate students were involved with the acquisition of all of these data. One was supported by the AOE Department until May 15, 2002 and the second was supported by this grant. Both of these students are now supported by this grant. A third student who was not supported by this grant helped obtain the surface pressure data.

This group again obtained access to the cascade tunnel in December 2002 until March 2003. After examining the endwall pressure data that were obtained earlier in 2002, it was decided to obtain more complete sets of surface pressure data in order to have lower uncertainty pressure gradient information. This is important for understanding how the pressure gradient affects the surface skin friction and the rapid distortion of the turbulence within the gap.

During this period, some data were obtained for the moving wall cases. Prior to these experiments, the proposed hardware improvements to the cascade facility were made in order to improve the LDV data rate, the mylar belt life, and the ability to get nearer to the wall for the moving wall cases. A new moving belt bed was designed and constructed for use with the Teflon pads and suction to eliminate the Teflon particles. The "Sure Tracker" was incorporated into the moving belt system to automatically keep the belt from moving laterally and prevent the scratched part of the Mylar belt from being in the field of view of the LDV. The use of this automatic belt tracking system will not only eliminate the scratching of the belt over the zone of measurements, but also eliminate the current need for a second person to be continually adjusting the belt roller. The "hot-air joint" scheme was used to improve the belt life. Unfortunately, all of the efforts to obtain LDV data through the transparent moving wall were only partly successful.

It was decided to implement the new Comprehensive LDV design in the future, which is briefly described below, in order to avoid trying to obtain LDV data through a moving wall. The Comprehensive LDV can obtain the vector velocity and position of a given particle within 10 microns uncertainty for a large 20 inches focal length optical system.

Progress During the 5th Year, 3/1/03 to 9/30/03

Because of the need to use the Comprehensive LDV in future moving wall measurements, it was decided to spend the time thoroughly analyzing the data from the non-moving wall cases and finishing the MS Thesis of Q. Tian and the Ph.D. dissertation of G. Tang. The hope is that additional funding after 10/03 will permit Q. Tian to modify and use the Comprehensive LDV for the moving wall experiments.

Discussion of some of the results for the non-moving wall cases are presented here. Considerable detail is given in the thesis and dissertation underway.

Flow Structure in the Linear Cascade Tunnel

From the oil flow visualization on the end wall (figures 10 and 11), and on the blade surface (figure 14), the tip leakage vortex and the passage vortex and secondary vortex can be found. From the LDV measurements, tip leakage vortex and separation on the blade tip surface and vortex sheet on the end wall and on the blade tip can be captured. Figure 13 presents a multiple tip vortex structure based on the oil flow visualization and LDV measurement.

Tip gap flow inside the blade passage, near the pressure side, is strongly accelerated in to the tip gap. This can be seen clearly from the oil flow visualization on the endwall (figure 10 and 11) and also the LDV measurement (figure 12, 13). The crossing point of the

blade surface and the dividing stream surface between the fluid, which is swept into the gap and that which is driven across the passage changes with the tip gap thickness. In the oil flow visualization figures, the tip gap flow is seen to leave the tip region approximately X/Ca=0.14 for t/c=1.65%, but for t/c=3.3%, X/Ca=0.38.

Cascade blades generally have a sharp corner at the entrance to the gap. Therefore, a separation vortex forms at the corner. Since there is no flow visualization on the blade tip, this feature can only be found in the LDV measurements in figure 3 and figure 4. Kang & Hirsch (1996) have reported separation vortices on the blade tips of the compressor blades in their cascade measurement and also presented that there are quite high shear stresses on the blade tip in the region next to the separation vortex. This high shear stress is accompanied by correspondingly high levels of convective heat transfer. This may help explain the "burn out" which sometimes occur in the region on the actual turbine blades.

As described in previous discussion, there are two basic flows in this cascade inner flow; one is the passage flow along the passage between the blades, the other one is the cross flow under the tip gap, mainly driven by the pressure difference between the blades. These two different flows meet together on the suction side of blade and roll up, forming the tip leakage vortex. As shown in the oil flow picture, the tip leakage flow pushes the passage vortex away from the suction surface. There is strong interaction between the tip leakage vortex and the passage vortex, resulting in the engulfment of the passage vortex. This interaction leads to considerable mixing as well as turbulence production, which ultimately results in loss production.

So far, we can see similar structural features of these two different tip gap flows for a stationary wall: a passage flow, a tip gap cross flow, a region of high wall shear stress under the blade tips, and the separation line associated with the tip leakage vortex. The qualitative nature of these two high shear stress regions is similar to some extent. The periodicity of the cascade is visible, and the flow is at an angle of approximately 90 degrees to the chord line of the blade, through the tip gap region for both inflow cases.

6

There are differences between the two tip gap flows (figures 10, 11, 15, 16, 17). From the oil flow visualization figures, the tip gap flow is seen to leave the tip region approximately at X/Ca=0.14 for t/c=1.65%, but for t/c=3.3%, at X/Ca=0.38. It means increasing tip gap, the separation line and tip leakage vortex move toward downstream. Assuming Z is the distance from the separation line to the blade along the z direction in the bed coordinate system, from the table1, in the same cross section, the separation line of the 1.65% case is much far away from the blade than that in the 3.3% case at the same cross section. It also implies 1.65% case has a stronger cross flow than 3.3% case. Since increasing the thickness, the cross flow endures a longer distance from pressure side to the suction side and will lost more kinetic energy. Relatively, the cross flow becomes weaker and passage flow becomes relatively stronger. The passage flow pushes the tip leakage vortex toward downstream.

Table1: Location of separation line relative to the blade surface

X (cm)	Z (cm)	
	t/c=3.3%	t/c=1.65%
5.791	1.217	5.444
6.672	2.807	6.257
7.379	4.192	6.878
8.172	5.277	7.417
8.966	6.485	8.182

Figures 19 and 20 show the Cp contours for the 2 tip gap flows. Figure 21 shows that the Cp at the mid-span of the blade is considerably different from the endwall Cp for the 3.3% tip gap case. Figures 22 and 23 show both the pressure gradient direction and relative magnitude, but the pressure level too. Figures 24 and 25 show the magnitudes of thje wall friction velocity computed from the near-wall sublayer LDV data and the measured pressure gradients.

References (Publications Produced During this Research Labeled with *):
Devenport, W.J. 1998/1999/2000, "Characterizing the unsteady vortical flow generated downstream of the tip of an axial pump rotor blade," related proposal and Annual Report to ONR.

Glegg, S.A.L., 1999, "The Response of a Swept Blade Row to a Three-dimensional Gust," *J. Sound and Vibration*, Vol. 227(1) pp.27-64.

*Kuhl, D.D. and Simpson, R.L. 2000 "Near-wall investigation of a streamwise vortex pair," paper 27.1, *10th International Symposium on Applications of Laser Techniques to Fluid Mechanics*, Lisbon, PT, July 10 – 13.

*Kuhl, D.D. and Simpson, R.L. 2001 "Near-wall Investigation of Three-dimensional Turbulent Boundary Layers," VPI-AOE-273, submitted to DTIC; also MS Thesis, D.D. Kuhl.

*Tang, Genglin 2004 "Measurements of the Tip Gap Turbulence Structure for a Stationary End-wall in a Low-Speed Compressor Cascade," Ph.D. dissertation, Aerospace and Ocean Engineering, Virginia Polytechnic Institute and State University.

*Tang, G., Simpson, R.L., and Tian, Q., 2004 "Measurement of the Tip Gap Turbulence Structure for a Stationary End-wall in a Low-Speed Compressor Cascade," to be submitted to AIAA Journal.

*Tian, Q. and Simpson, R.L. 2003 "Some Features of the Tip Gap Flow Fields of a Linear Compressor Cascade," VPI-AOE-286, submitted to DTIC; also MS Thesis, Q. Tian.

*Tian, Q., Simpson, R.L., and Tang, G. 2004 "Surface Oil Flow Visualization in the Linear Compressor Cascade with Tip Leakage," submitted to *Measurement Science and Technology*. (ATTACHED)
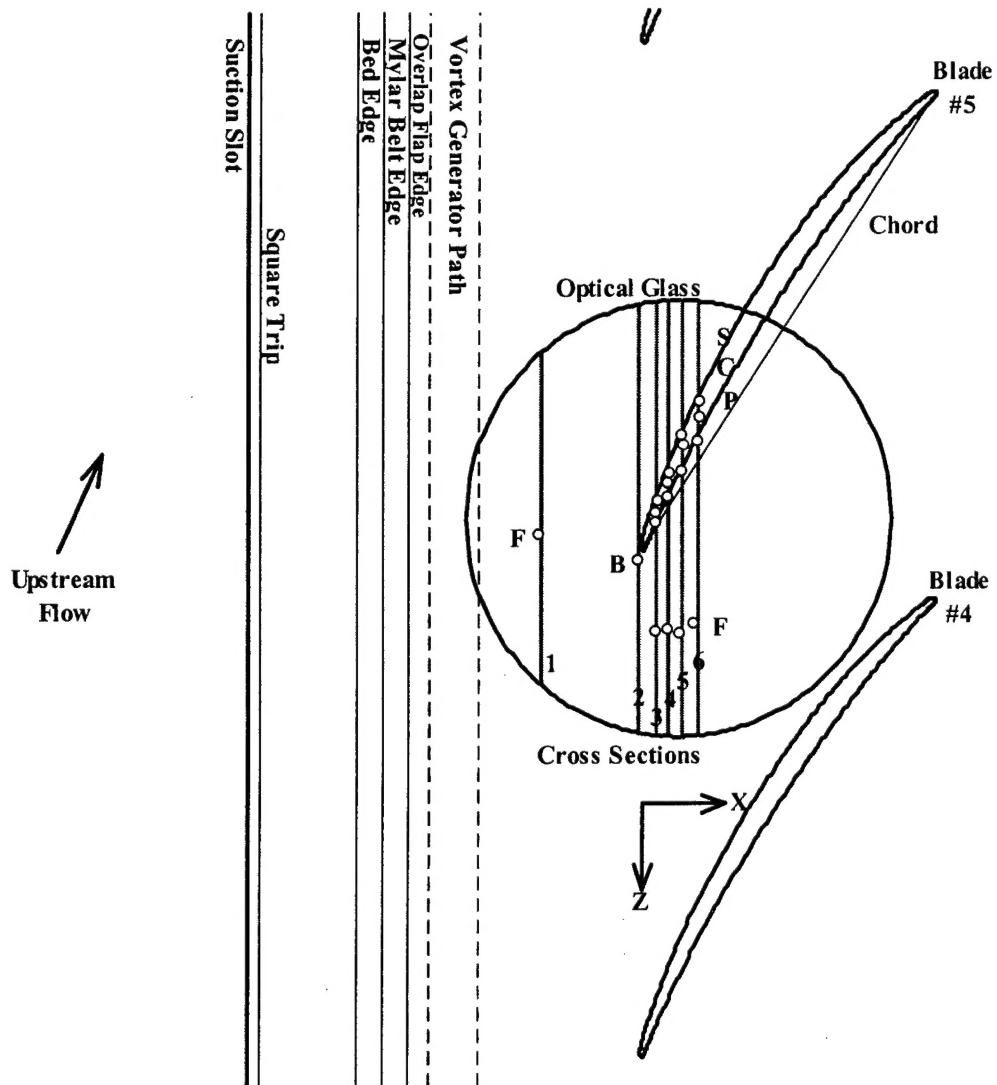
FIGURE 1A: STATIONARY WALL MEASUREMENT POINTS TAKEN BY KUHL (2001) FOR X/C < 0.25.

FIGURE 1b   COORDINATE SYSTEM AND BLADE GEOMETRY

10
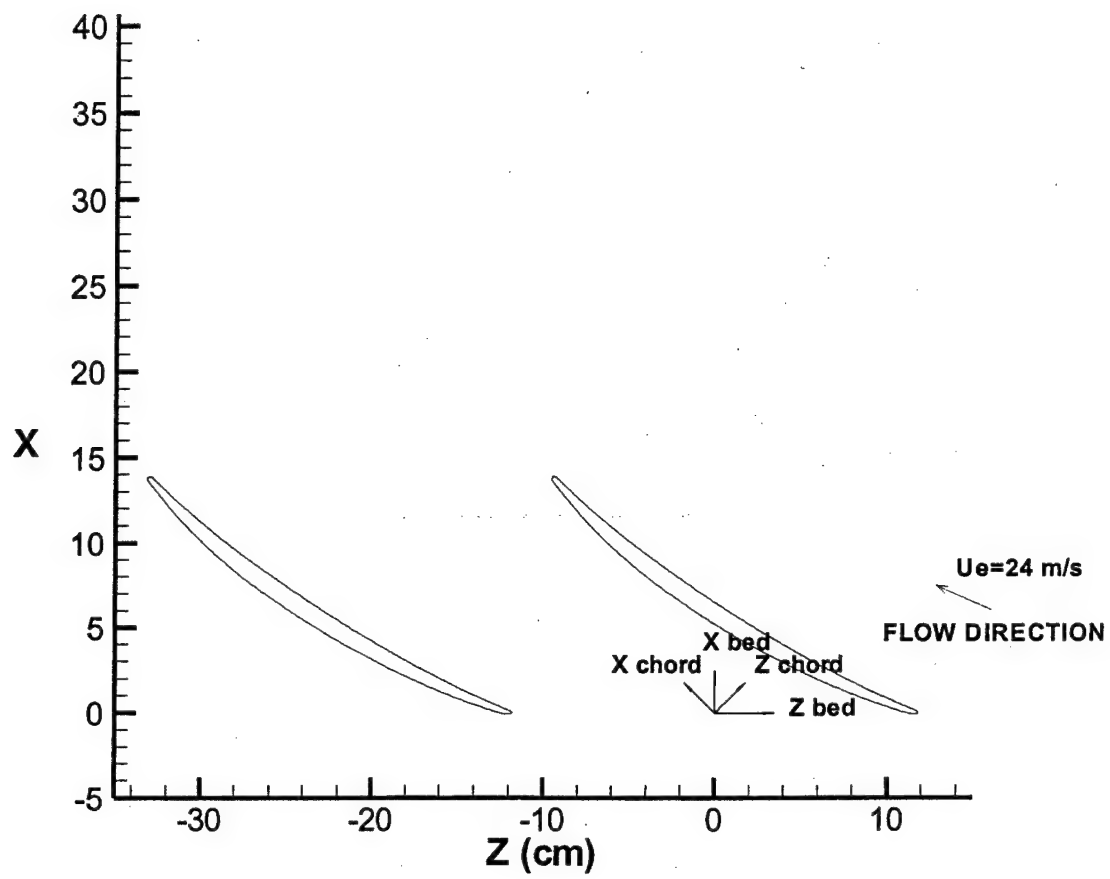
FIGURE 2   UW VECTOR PLOT IN BED COORDINATE SYSTEM
FOR STATIONARY WALL WITH TIP GAP 1.65%
(Black represents Hot Wire Data)
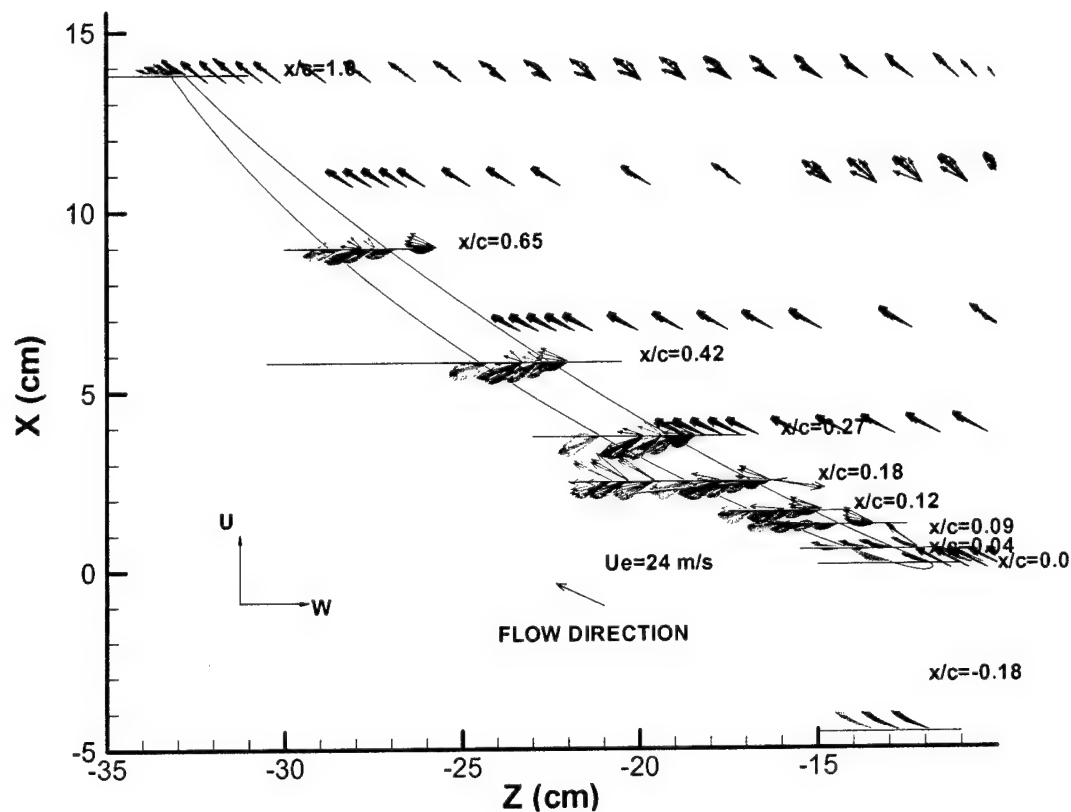
FIGURE 3   UW VECTOR PLOTIN BED COORDINATE SYSTEM
FOR STATIONARY WALL WITH TIP GAP 1.65%
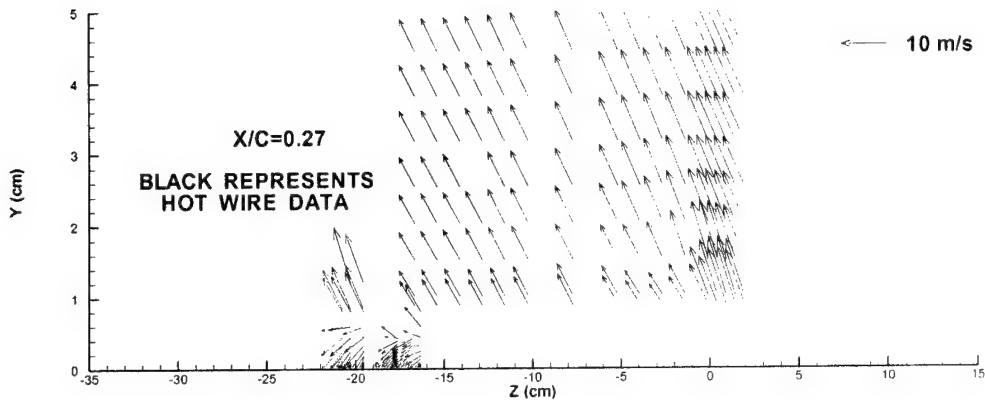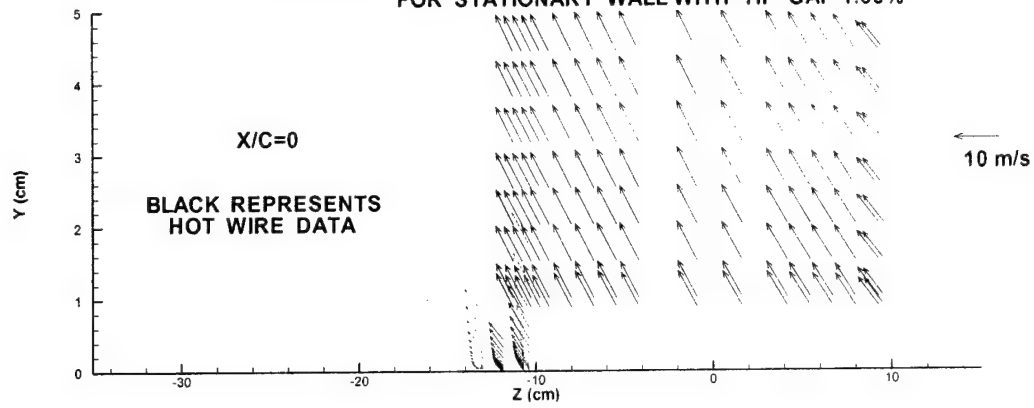(Black Represents Hot Wire Data)
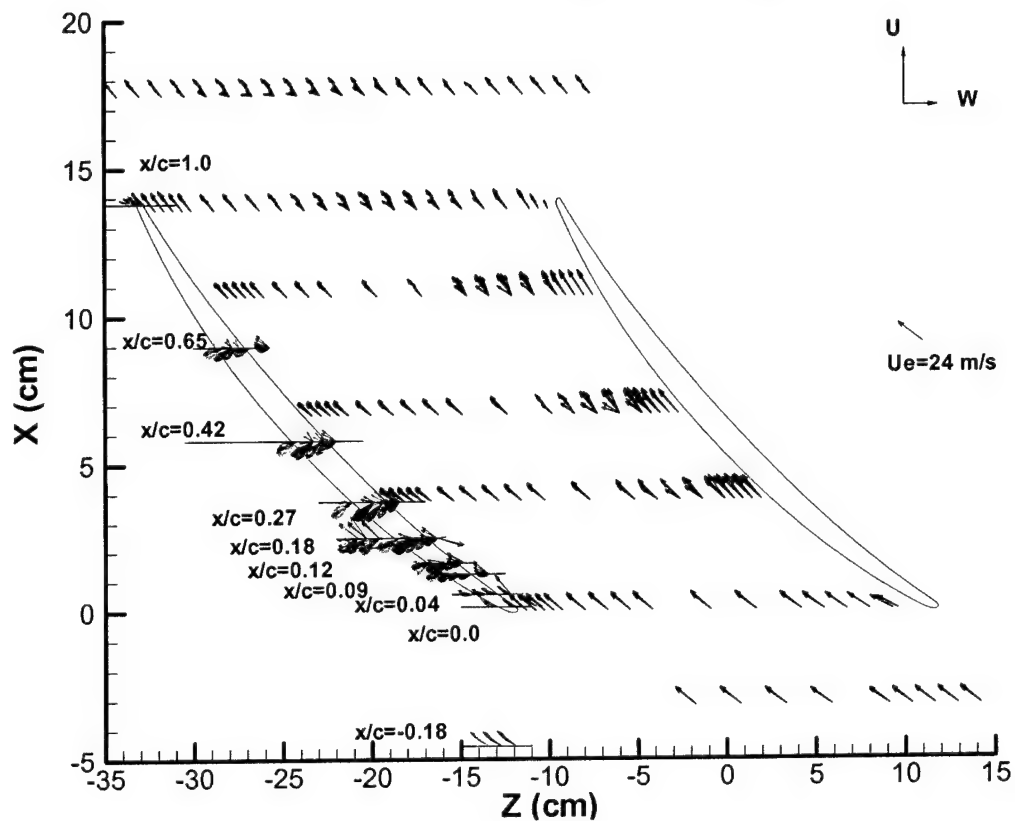
FIGURE 4 VW VECTOR PLOT IN BED COORDINATE SYSTEM
FOR STATIONARY WALL WITH TIP GAP 1.65%

FIGURE 5 UW VECTOR PLOT IN BED COORDINATE SYSTEM FOR STATIONARY WALL WITH TIP GAP 1.65%
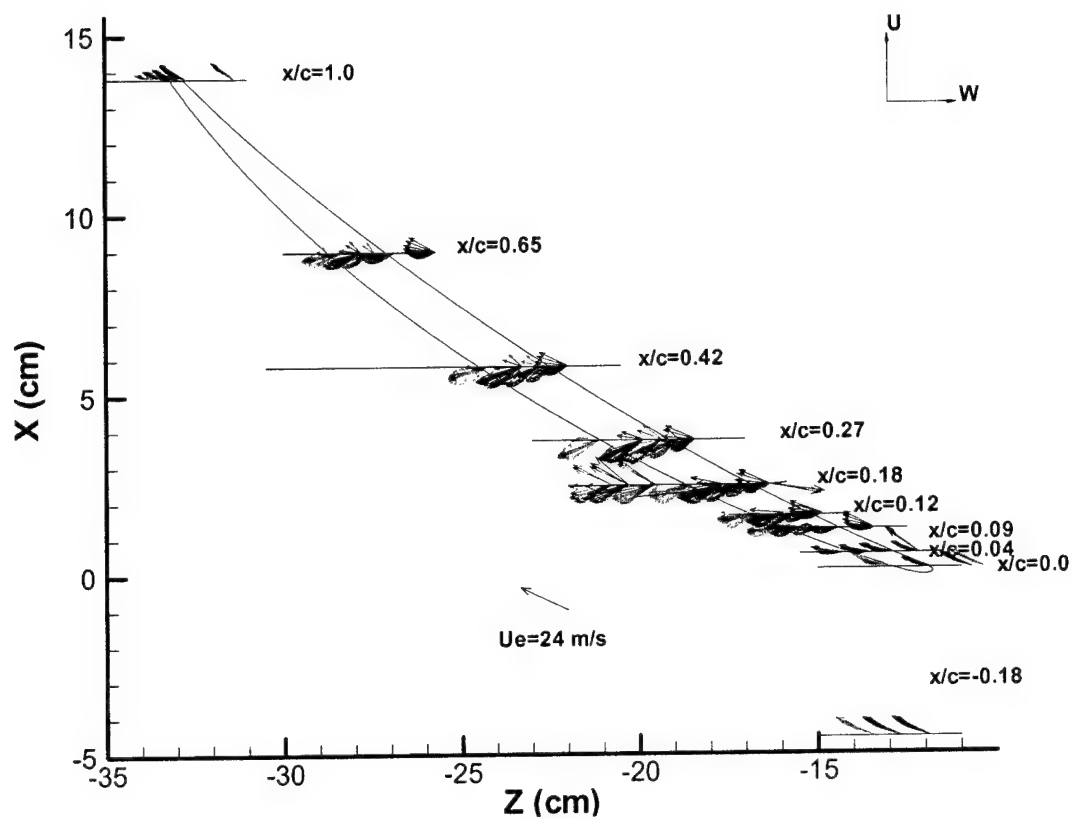
FIGURE 6 UW and VW PLOTS IN BED COORDINATE SYSTEM WITH TIP GAP 1.65%
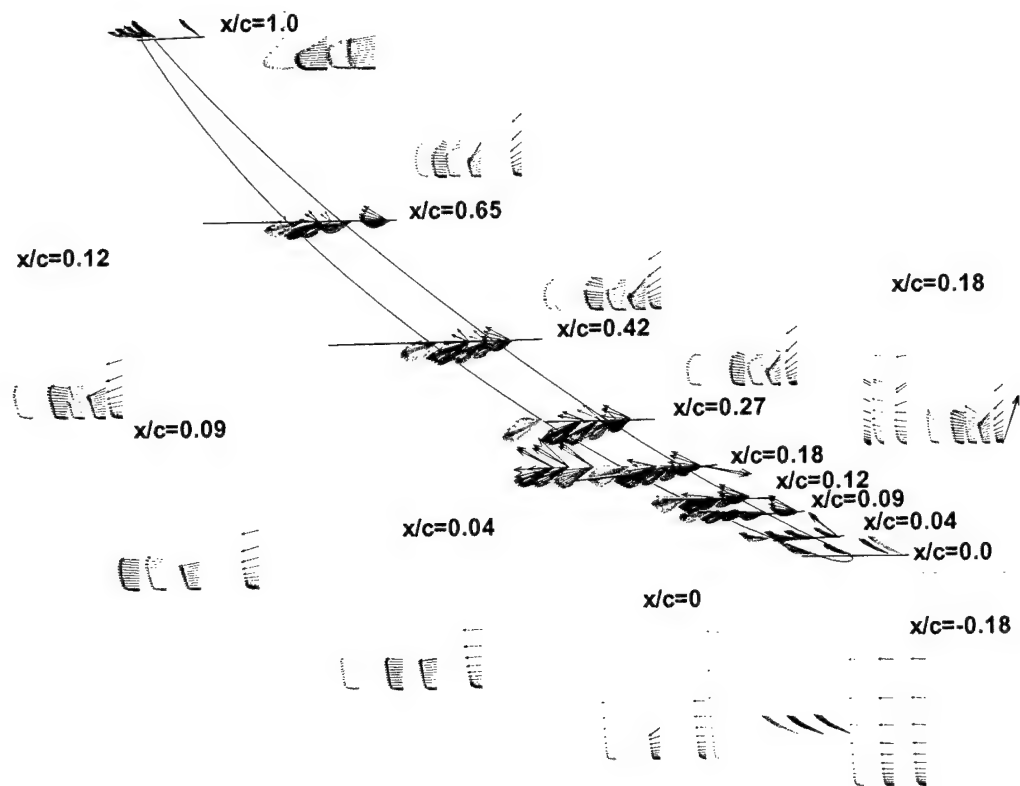
FIGURE 7

VW Vector plots
in chord coordinate system
for stationary wall with 1.65%

x/c=-0.18

x/c=0.0

x/c=0.04

x/c=0.09

x/c=0.12

x/c=0.18

x/c=0.27

x/c=0.42

x/c=0.65

x/c=1.0

16

FIGURE 9

VW Vector plots
in chord coordinate system
for stationary wall with 3.3%

x/c=-0.18

x/c=0.0

x/c=0.04

x/c=0.09

x/c=0.12

x/c=0.18

x/c=0.27

x/c=0.42

x/c=0.65

x/c=1.0

V

W

Flow
direction

Tip leakage
vortex from
blade 5

Tip leakage
vortex from
blade 4

Separation line between tip-
leakage vortex and the low wall
shear stress flow through the

High wall shear stress region under
the blade tip
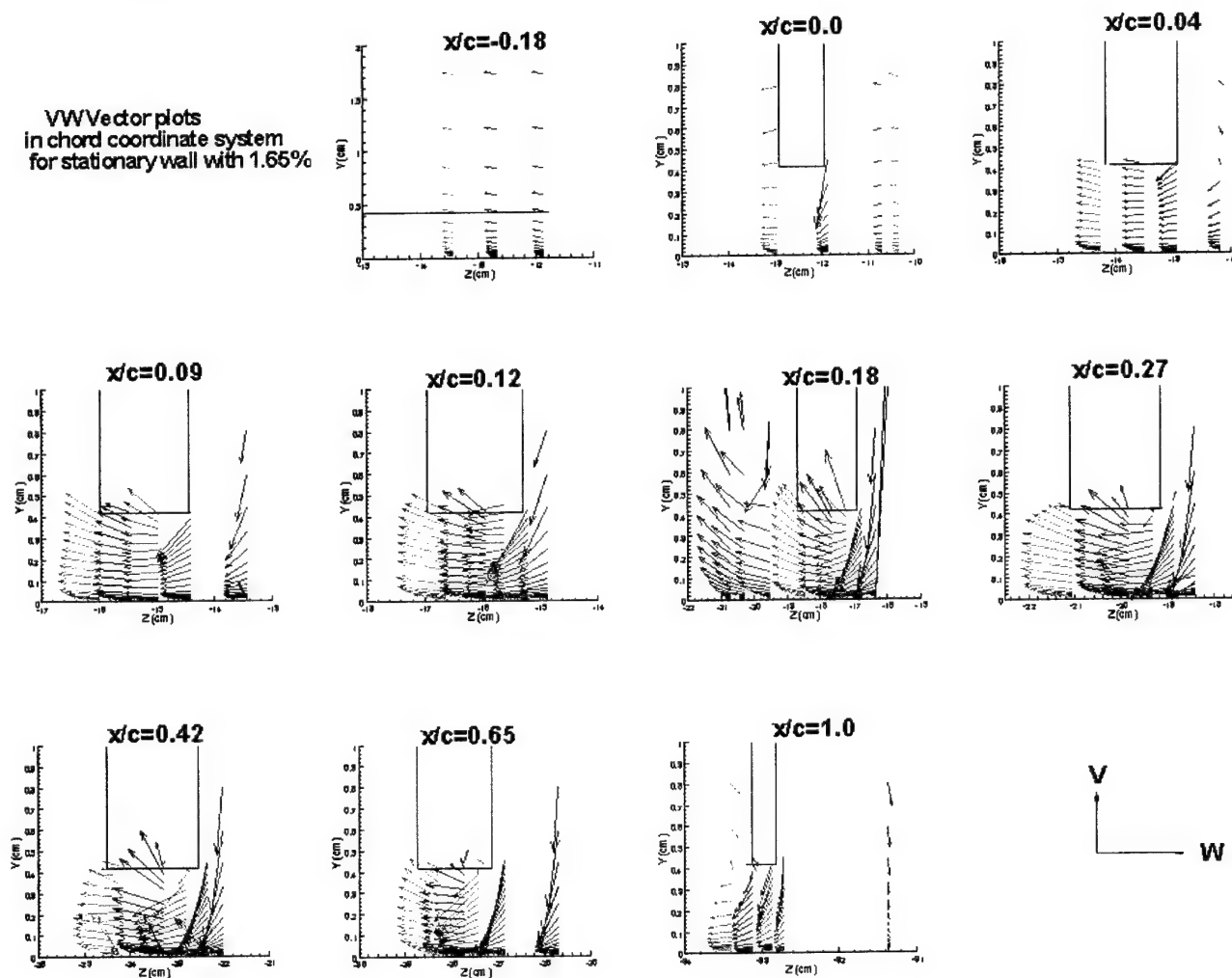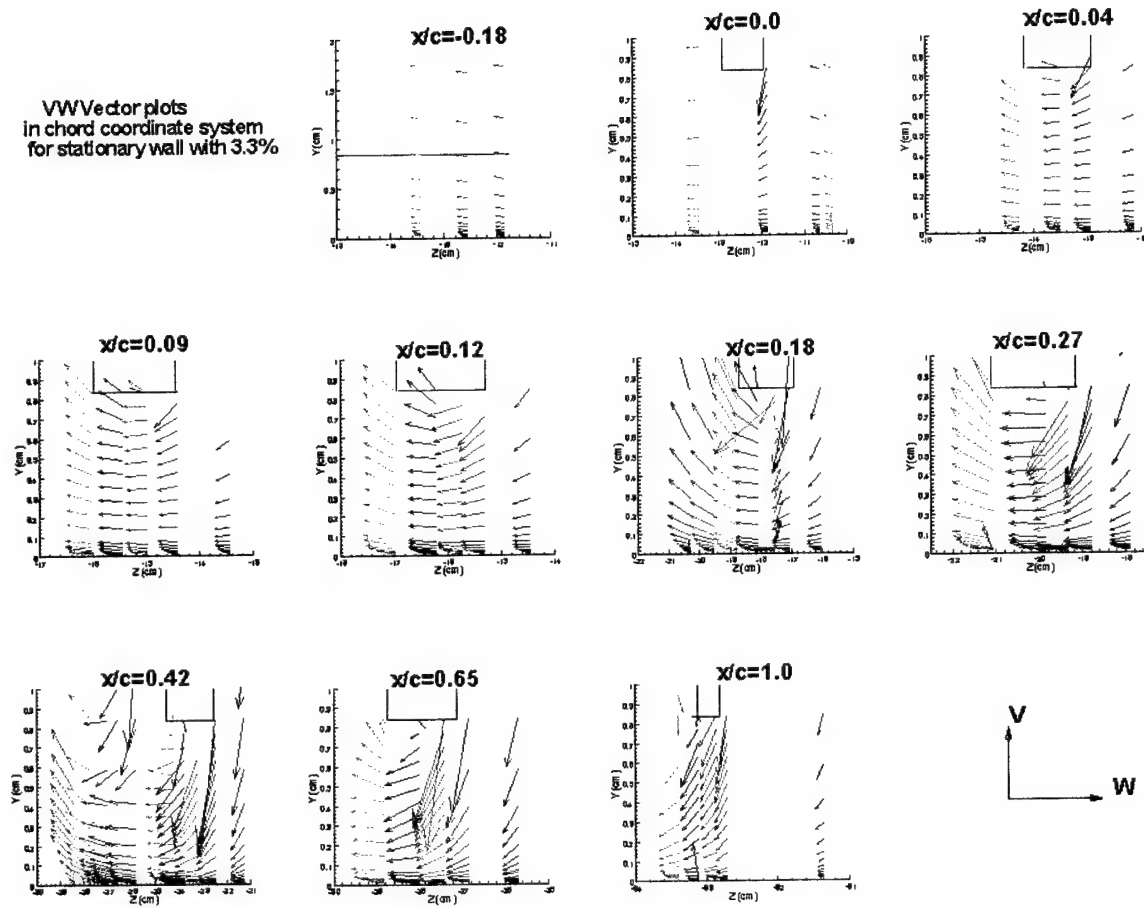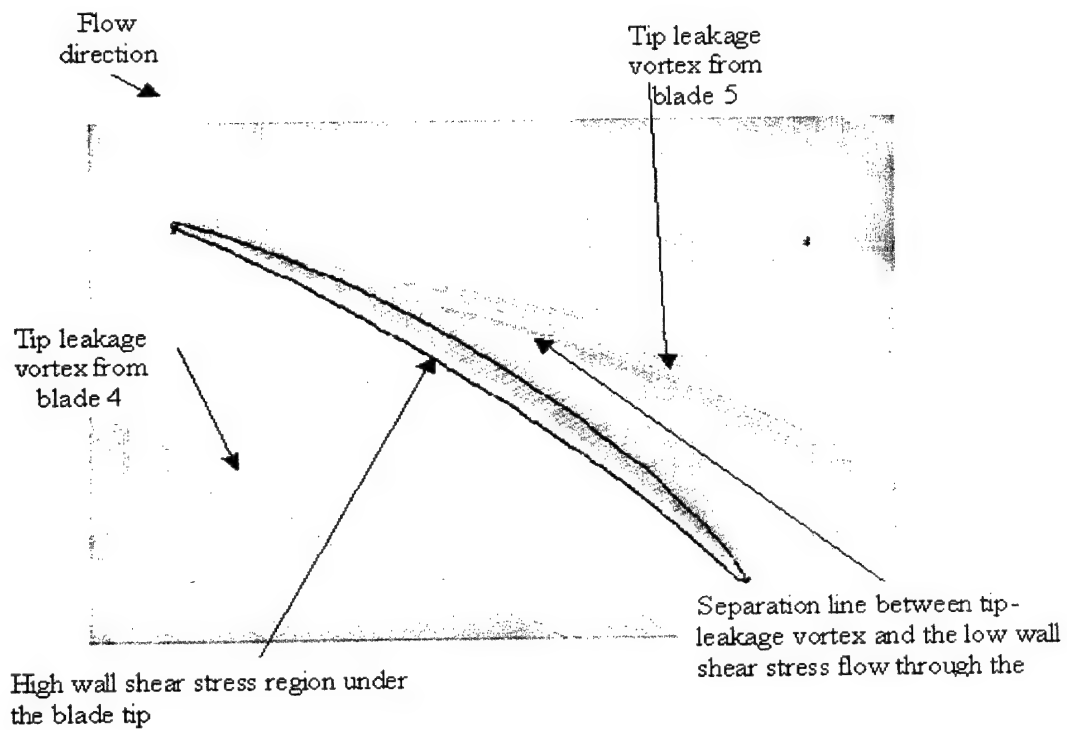
Figure 10. Oil flow visualization on the endwall (from Chittiappa Muthanna t/c=1.65%)

Flow direction

Tip leakage vortex
from blade 3

Tip leakage vortex
from blade 4

Separation line between tip-leakage vortex
and the low wall shear stress flow through the
passage

High wall shear stress region under the blade tips
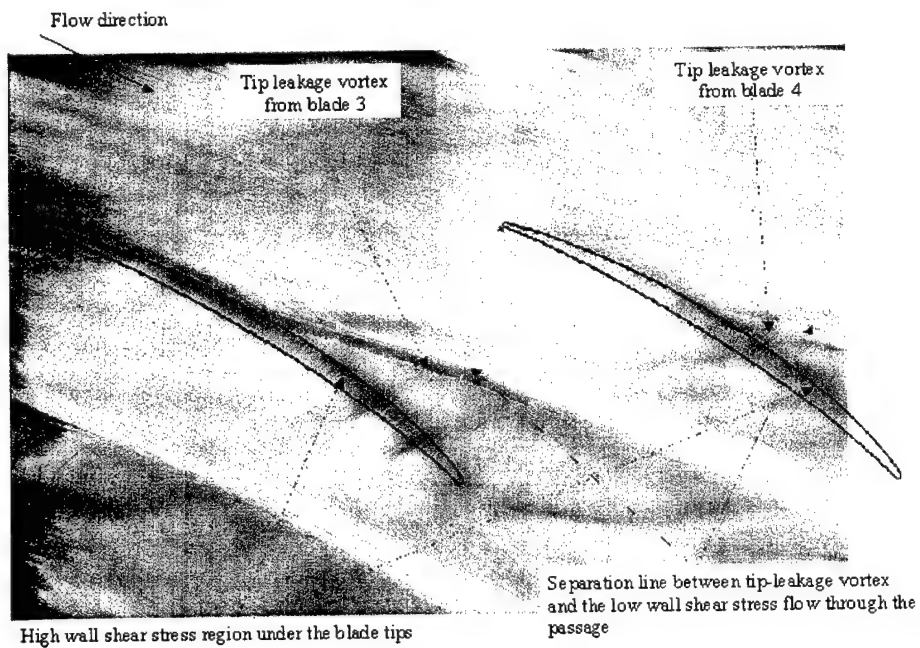
Figure 11. Oil flow visualization on the endwall (t/c=3.3%)
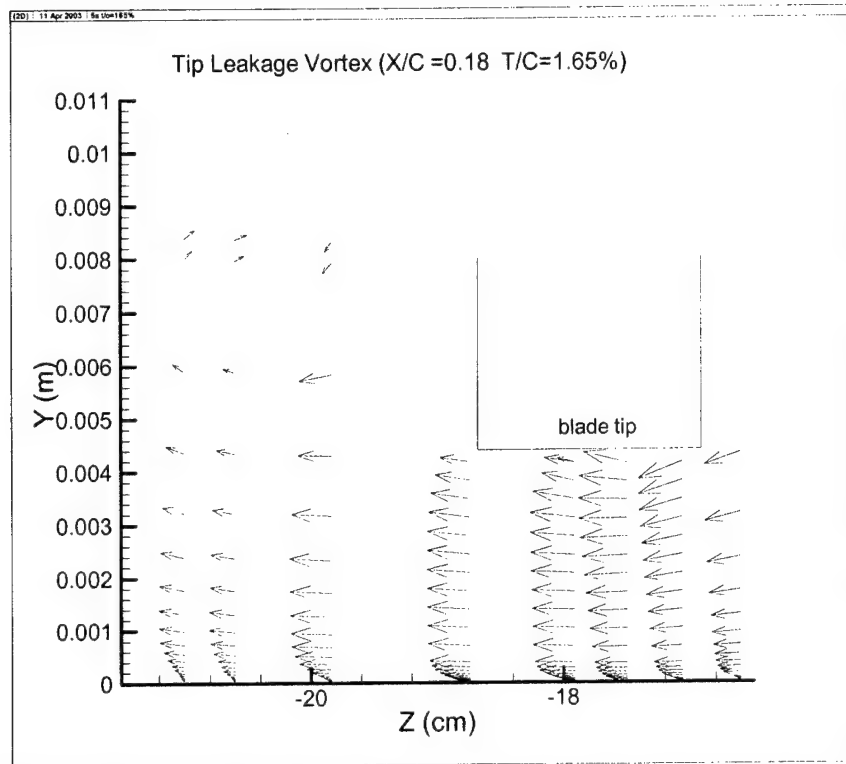
Figure 12. Mean velocity flow field in the tip gap and tip leakage vortex (t/c=1.65%) in the separation coordinates
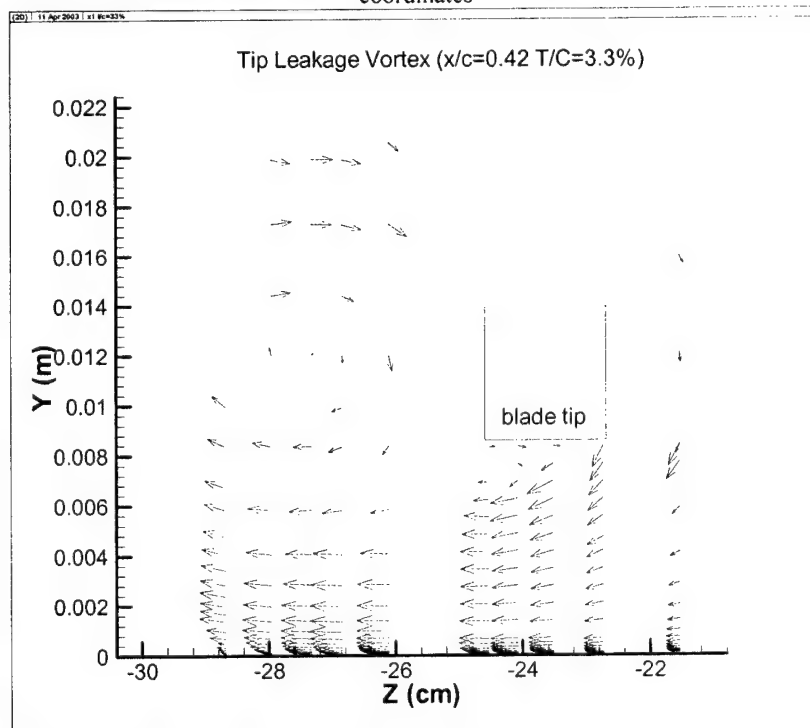
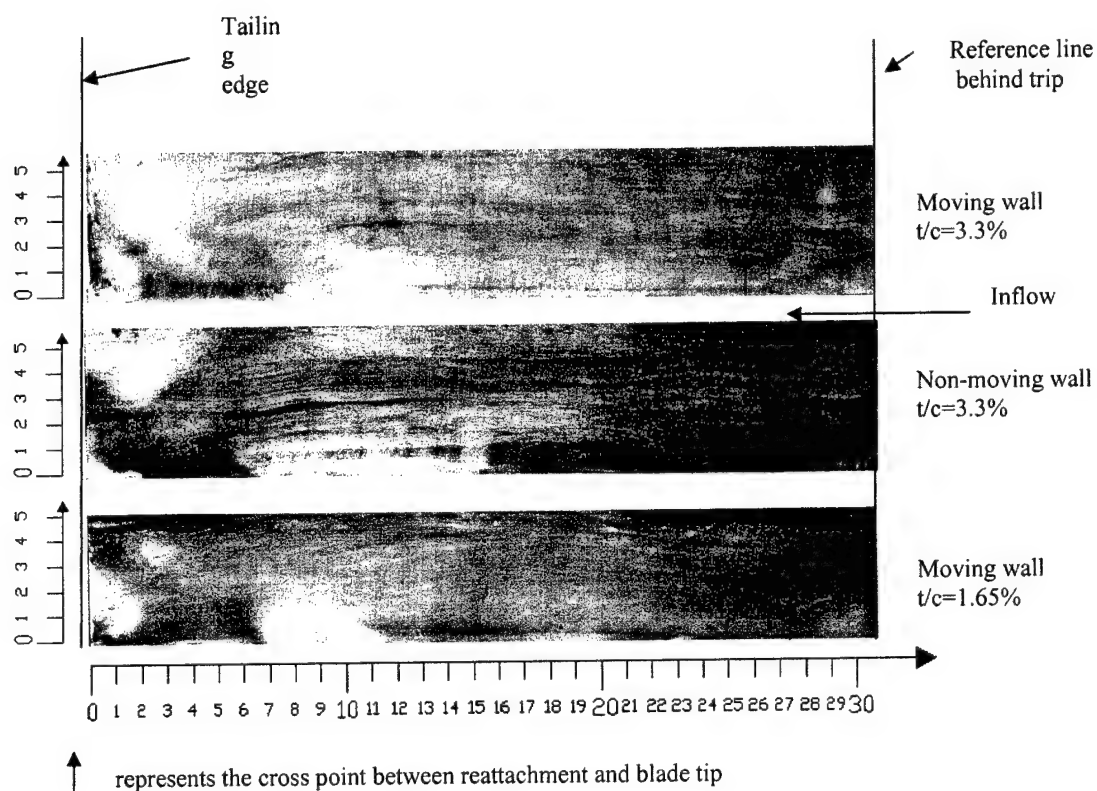Figure 13. Mean velocity flow field in the tip gap and tip leakage vortex (t/c=3.3%) in the separation coordinates

Tailing edge

Reference line behind trip

Moving wall t/c=3.3%

Inflow

Non-moving wall t/c=3.3%

Moving wall t/c=1.65%

0 1 2 3 4 5 6 7 8 9 10 11 12 13 14 15 16 17 18 19 20 21 22 23 24 25 26 27 28 29 30

↑ represents the cross point between reattachment and blade tip

Figure 14. Oil flow visualization on the blade surface.
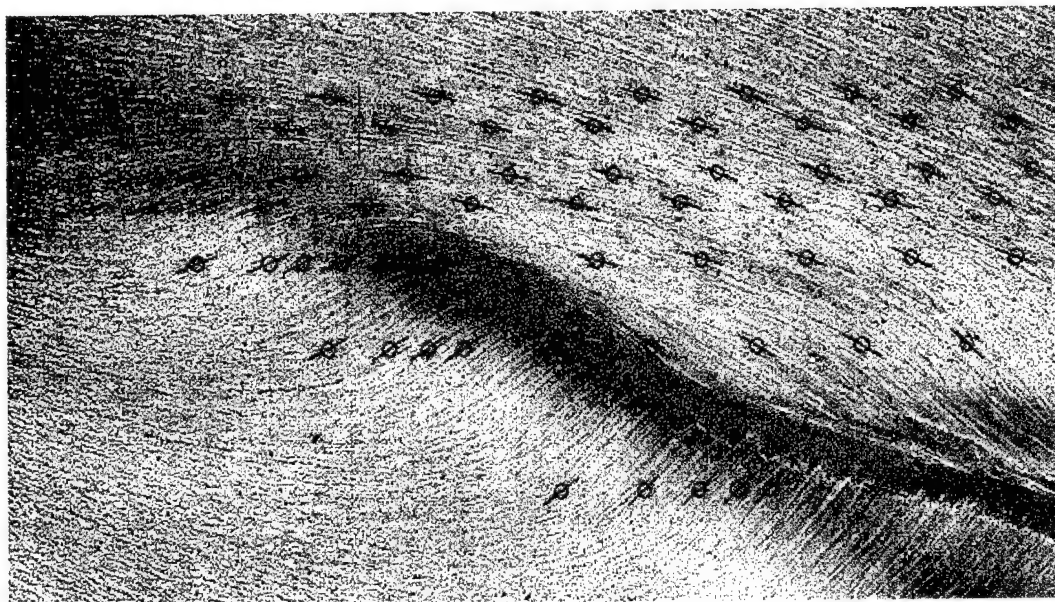
Figure 15.   Wall shear stress direction measurement using digitized oil flow pictures

20
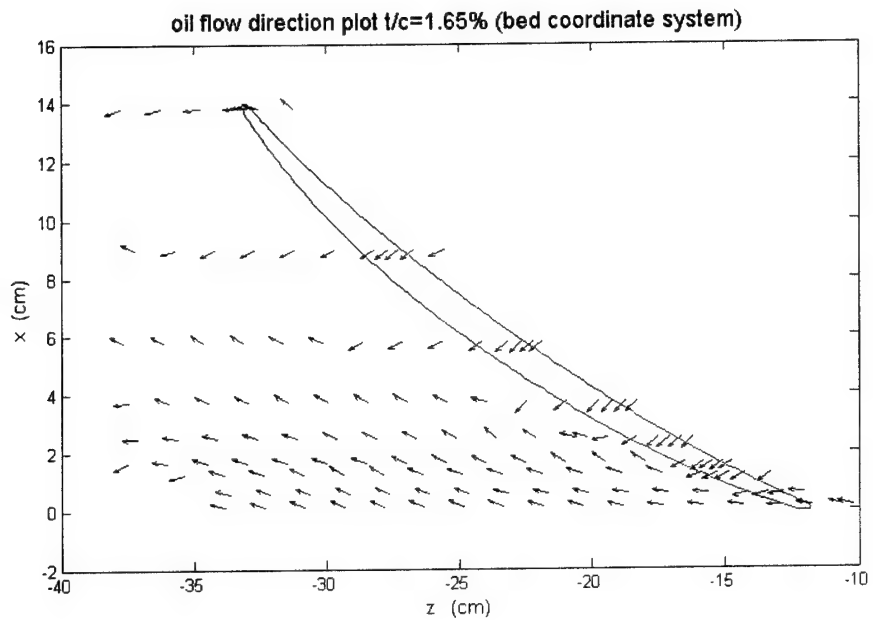
Figure 16. Wall shear stress direction t/c=1.65% (measured from the digitized oil flow pictures)
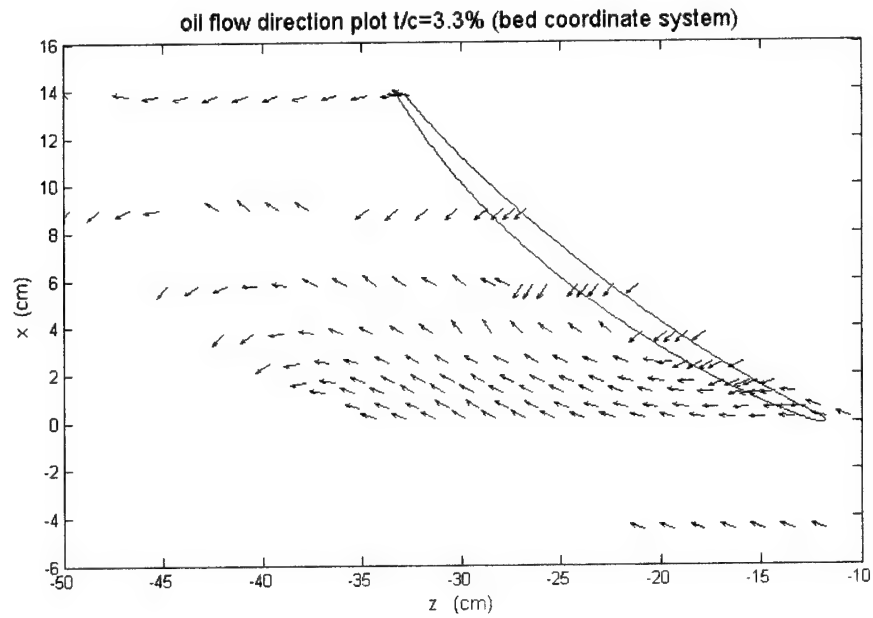
Figure 17. Wall shear stress direction t/c=3.3% (measured from the digitized oil flow pictures)

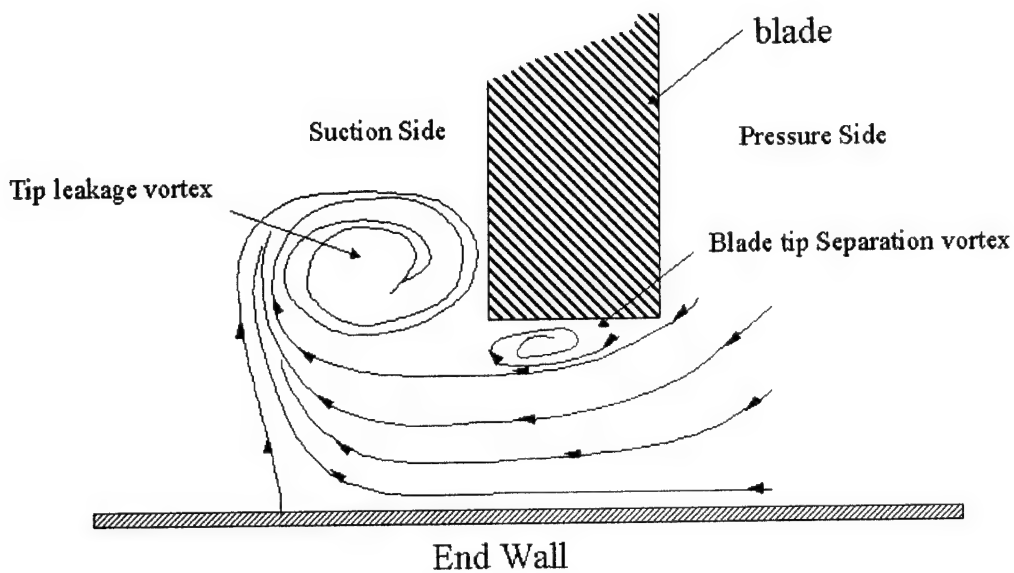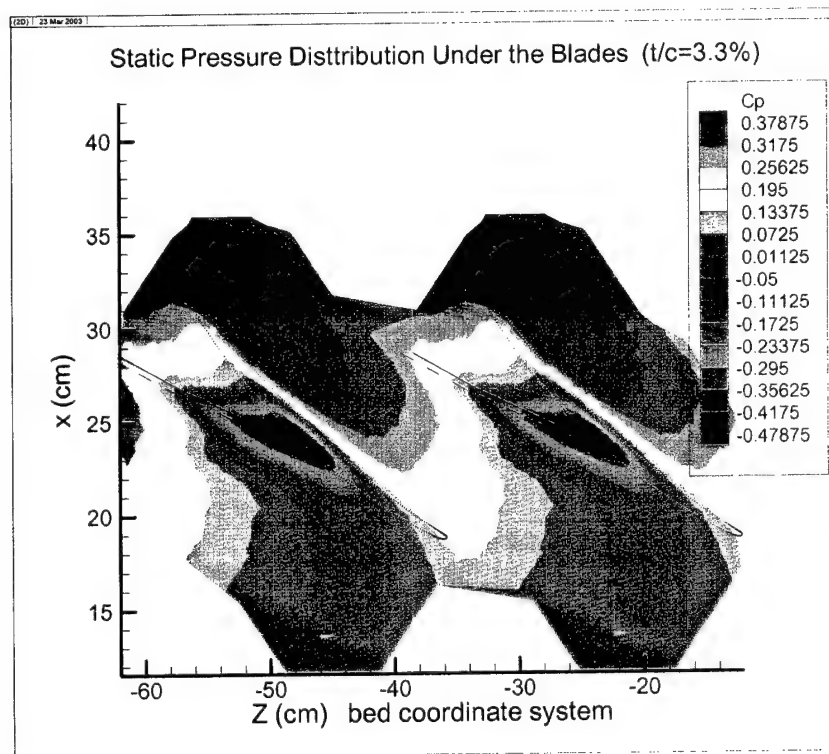Figure 18. Flow structure in the blade tip region.

FIGURE 19. CONTOURS OF STATIC PRESSURE COEFFICIENT MEASURED ON THE ENDWALL T/C=3.3%

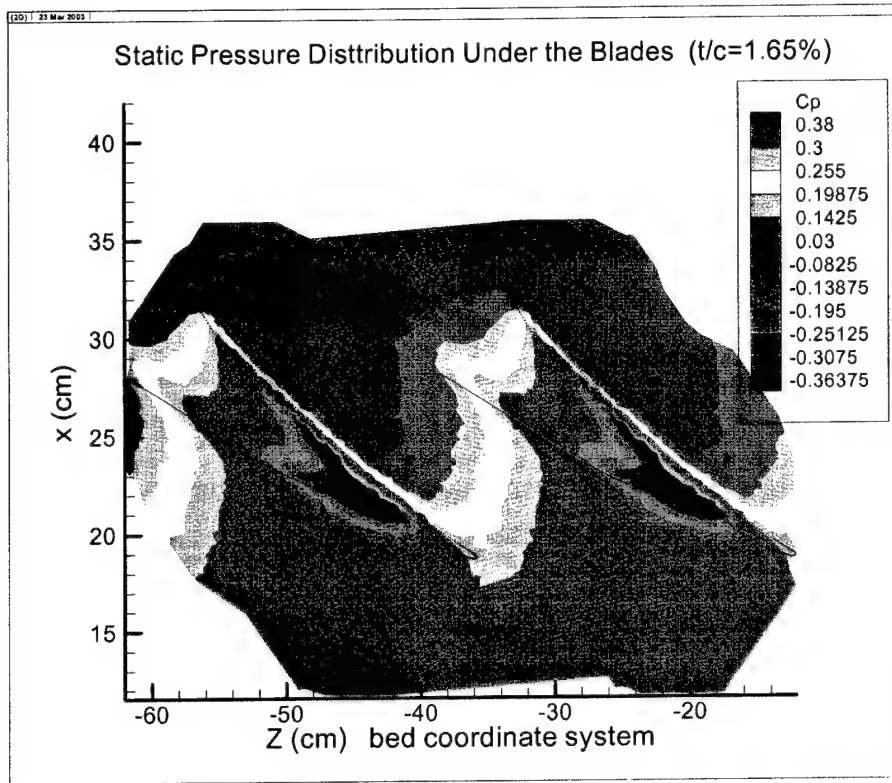DASH LINE IS THE CORRECTED SEPARATION AND SOLID LINE IS FROM THE OIL FLOW MEASUREMENT

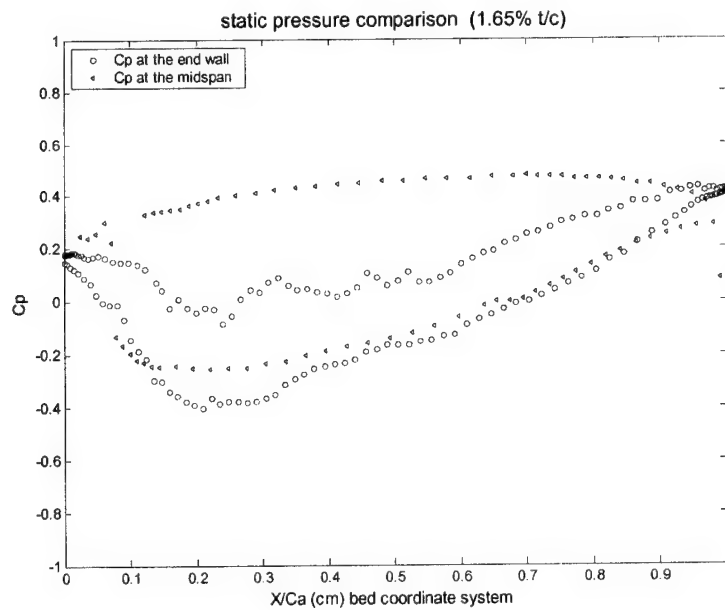Figure 20. Contours of static pressure coefficient measured on the endwall t/c=1.65%

Figure 21. Static pressure comparison on the endwall and on the mid span of the blade t/c=1.65% at blade contour locations
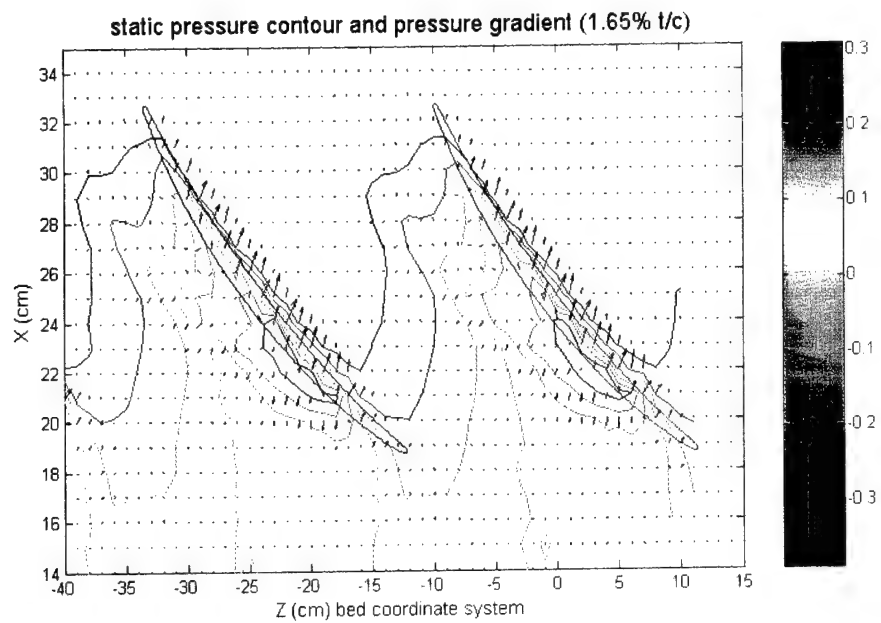
static pressure contour and pressure gradient (1.65% t/c)

Figure 22. Contours of static pressure Cp and pressure gradient vector plot t/c=1.65%

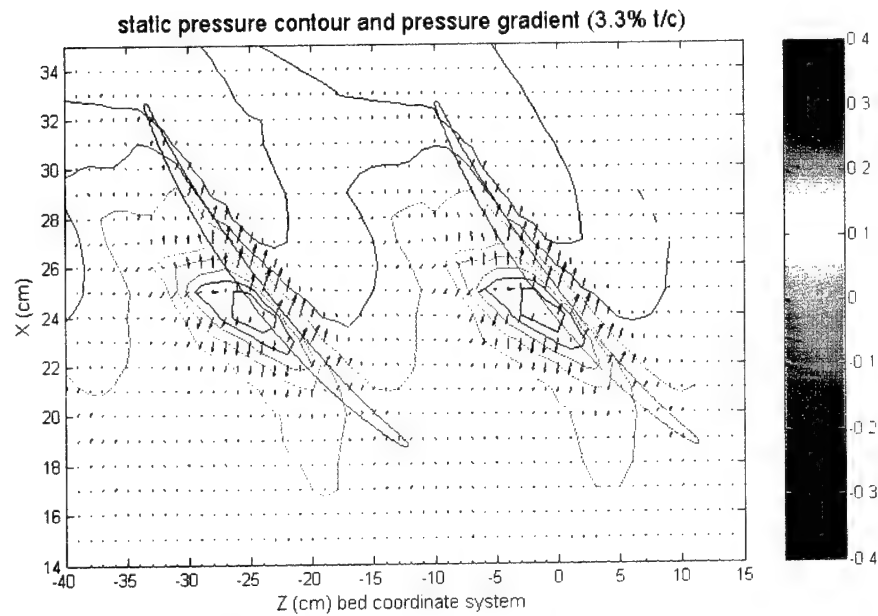### static pressure contour and pressure gradient (3.3% t/c)

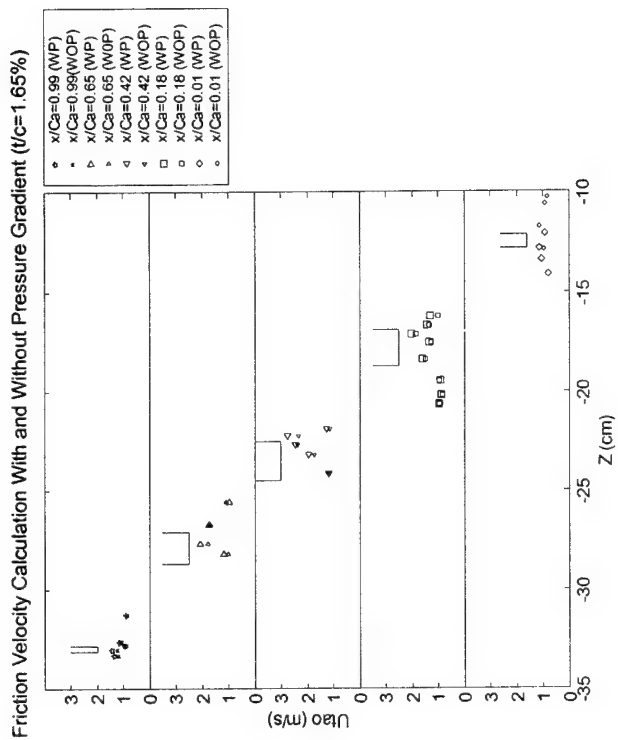Figure 23. Contours of static pressure Cp and pressure gradient vector plot t/c=3.3%

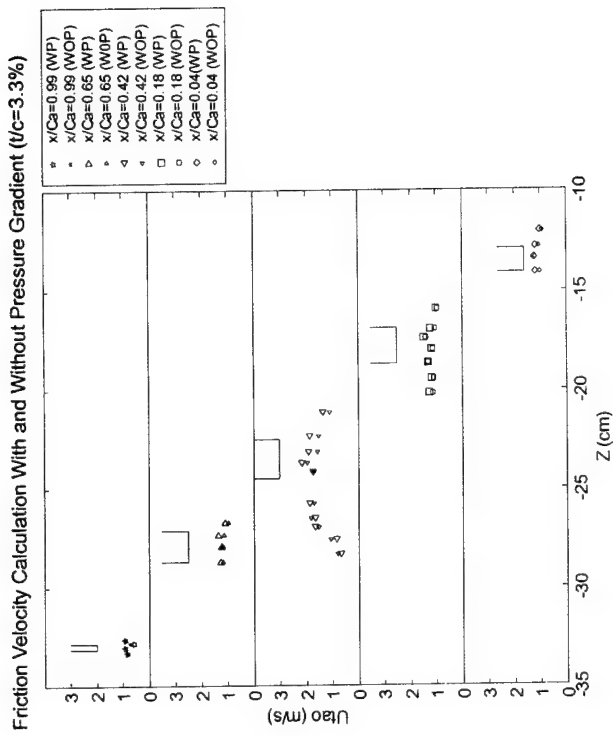Figure 24. Skin friction velocity comparison with and without pressure gradient t/c=1.65%

Figure 25. Skin friction velocity comparison with and without pressure gradient t/c=3.3%

26

Surface oil flow visualization in the linear compressor cascade with tip leakage

Qing Tian*, Roger L. Simpson†, and Genglin Tang*

Department of Aerospace and Ocean Engineering, Virginia Polytechnic Institute and State University, Blacksburg, VA 24061, USA

† Jack E. Cowling Professor, Department of Aerospace and Ocean Engineering, 215 Randolph Hall, Fellow AIAA
† Corresponding author. Email address: simpson@aoe.vt.edu
*Graduate student, Research assistant, Department of Aerospace and Ocean Engineering

ABSTRACT

Surface oil flow visualizations were conducted in the VPI&SU Dept. of AOE Low Speed Linear Cascade Wind Tunnel on the end wall. Oil flow visualizations of the end wall flow features (passage flow, cross flow and tip leakage vortex) for tip gap to chord ratio of $t/c=1.65\%$ and 3.3% are discussed in detail. For the first time, quantitative comparisons are made between the oil-flow direction and the wall shear stress direction obtained from laser Doppler anemometer experimental results. The oil flow streaks are aligned with the wall shear stress direction, except near separation, which is proved theoretically and experimentally. Wall shear stress directions in the oil-flow images are measured and the separation line in the oil flow is calibrated based on the skin friction results from the LDA measurement.

Keywords: oil flow visualization, LDA, wall shear stress, linear compressor cascade, flow angle.

1 INTRODUCTION

The main goal of this study of the flow through a linear compressor cascade is to obtain greater insights into the complex flow through turbo-machinery. Through experimental study, more accurate computational models can be developed with the resulting benefit of better initial designs of rotors. Research on the three-dimensional flow in axial flow turbo-machinery with a tip gap can be traced back to the 1920s, as reviewed by Prasad (1977). At the end of last century, due to the limitation of the experiment technology, most of the investigations on axial compressor flow fields were concerned with the rotor wake characteristics and
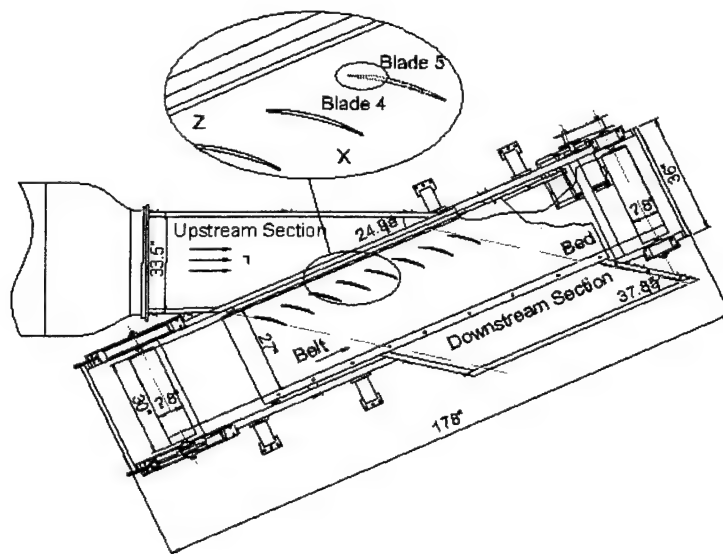
1

Figure 1. Test section of the linear cascade tunnel

with the interaction regions of the casing wall boundary layer. Currently, there are limited experimental data documenting the development of the tip leakage flow, wall shear stress measurement and the location of the separation line, which are associated with the tip clearance.

The present experimental studies have been conducted in a linear compressor cascade with the special emphasis on the tip leakage flow development near and in the tip clearance. A simultaneous three-orthogonal velocity component fiber optic laser Doppler anemometer (LDA), which is described by Chesnakas and Simpson (1994), and oil flow visualization technique are used to measure the near wall flow field. Comparisons are made quantitatively between the oil-flow direction and the wall shear stress direction from the laser Doppler anemometer results. One purpose of this paper is to provide a source of experimental surface oil flow measurements of the oil flow streaks angles and the separation lines on two different tip clearances with tip gap to chord ratios of 1.65% and 3.3%. Another more widely useful purpose is to show that the oil flow streaks are aligned closely with the direction of the skin friction vector, except near separation, and that the effect of the oil flow on the boundary layer motion is very small. The separation lines based on the oil flow visualization results are calibrated with the LDA results. This is the first known work that quantitatively shows the uncertainty of an oil

flow streak direction.

2 EXPERIMENTAL FACILITY
2.1 WIND TUNNEL AND TEST CONDITIONS

Experiment measurements were conducted in the VPI&SU Dept. of AOE Low Speed Linear Cascade Wind Tunnel. The drawing of the test section of this linear cascade is shown in figure 1. This wind tunnel has an open circuit and is powered by a 15 hp motor with a fan. Air from the fan is supplied to a test section after first passing through a diffuser, a series of flow conditioning screens, a section of honeycomb to remove the mean swirl of the flow, another series of flow conditioning screens, a contraction, and then into the test section. There are two three–quarter inch high suction slots on the upper and lower end wall at $0.19\ m$ in front of the cascades to remove the inlet flow boundary layer (see figure 2). The flow is tripped by a square bar mounted on the lower suction slot as shown in figures 1 and 2. The nominal running conditions are the speed of $25\ m/s$ and temperature of $25\ \text{\textcelsius}\pm1.0\ \text{\textcelsius}$. The test section consists of eight cantilevered GE rotor B section blades, a plywood bed with a Teflon cover, optical glass inserts, and a plexiglass roof. The entrance of the test section is a rectangular cross section of $1.651m\times0.254\ m$. Details of the aerodynamic design of the cascade are given in table 1 and by Muthanna, 1998. Eight blades were cantilevered on the beam, so they could be moved
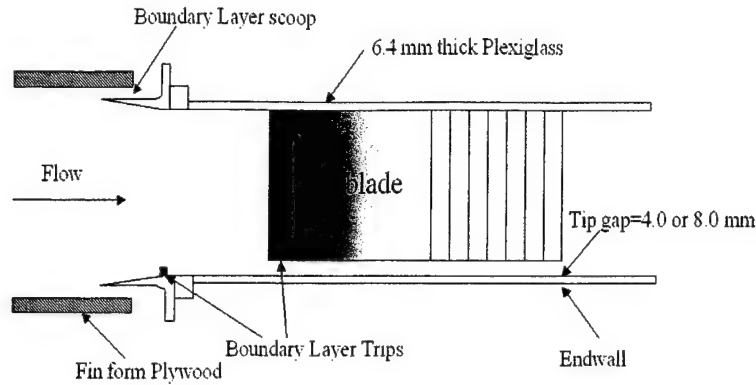
2

Figure 2. Side view of the test section of the linear cascade tunnel

Table 1. Parameters of the cascade blades

Blade section	GE rotor B section
Blade number	8
Chord length	25.4 cm
Inflow angle	65.1°
Stagger angle	56.9°
Pitch	0.929 of the chord
Span	1.0 of the chord
Axial Chord length	13.868 cm
Passage width	23.6 cm
Reynolds number based on the chord	4.03×10^5
Tip gap height	0.0165 of chord and 0.033 of chord

relative to the end-wall to vary the clearance gap at the tip by adjusting the fixture on the beam or add fixed washer between the beam and the tunnel frame. Two different tip leakage flows with tip gap to chord ratios of 1.65% and 3.3% are tested.

2.2 SURFACE OIL FLOW TECHNIQUE

Surface oil flow visualizations were done on the lower end-wall in the blade passage with two different tip clearances (t/c=1.65% and 3.3%) to investigate tip leakage flow. A black adhesive plastic sheet (47.5 *cm* ×27.5 *cm*×0.02 *cm*) was mounted under the tip gap on the end-wall. A mixture in a proportion of 15 ml. titanium dioxide powder, 40 ml. kerosene and 1ml. of oleic acid dispersant was painted with a brush on this black adhesive plastic sheet. In order to avoid possible static electricity generated from the oil brush and the

plastic, a thin aluminum foil was put under and above the plastic at the edge and grounded. The tunnel was run for about 5 minutes until all the kerosene evaporated, and then a fast drying lacquer was sprayed to the surface of the black plastic to preserve the traces. This black plastic was removed, and various details of this surface oil flow pattern were digitized by a scanner with 1000 *ppi* (Pixel Per Inch) resolution in the gray scale, and presented in figure 3 and figure 4. The movement of the oil mixture sheet driven by the flow and the formation of the oil flow streaks could be clearly revealed and recorded.

With these digitized oil-flow images, AutoCAD engineering design software was used to measure the directions of the local oil streaks on the oil-flow images. In figure 5, each circle center is a local point where the oil-flow streak direction is measured. In order to measure the oil flow direction, a line passing through the circle center is drawn tangent to the streaks. The angle between
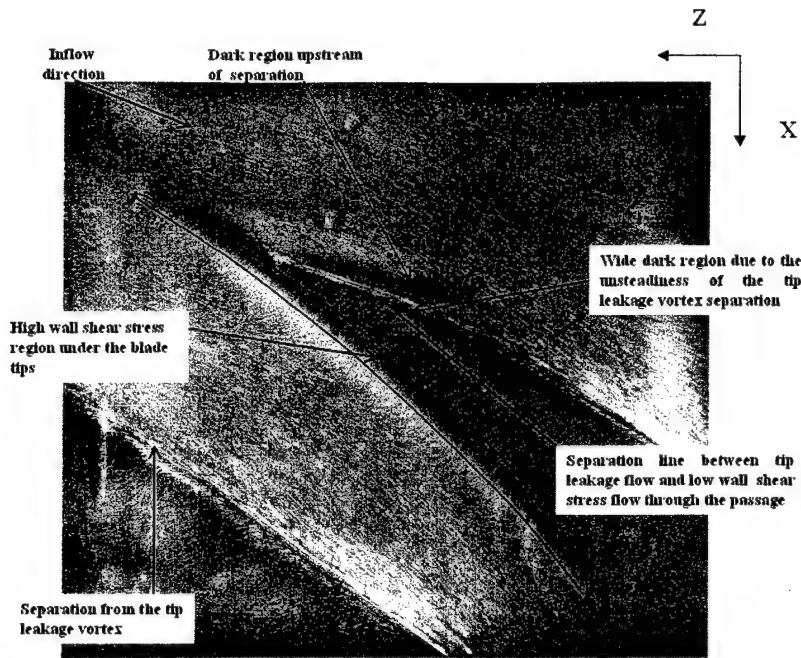
3

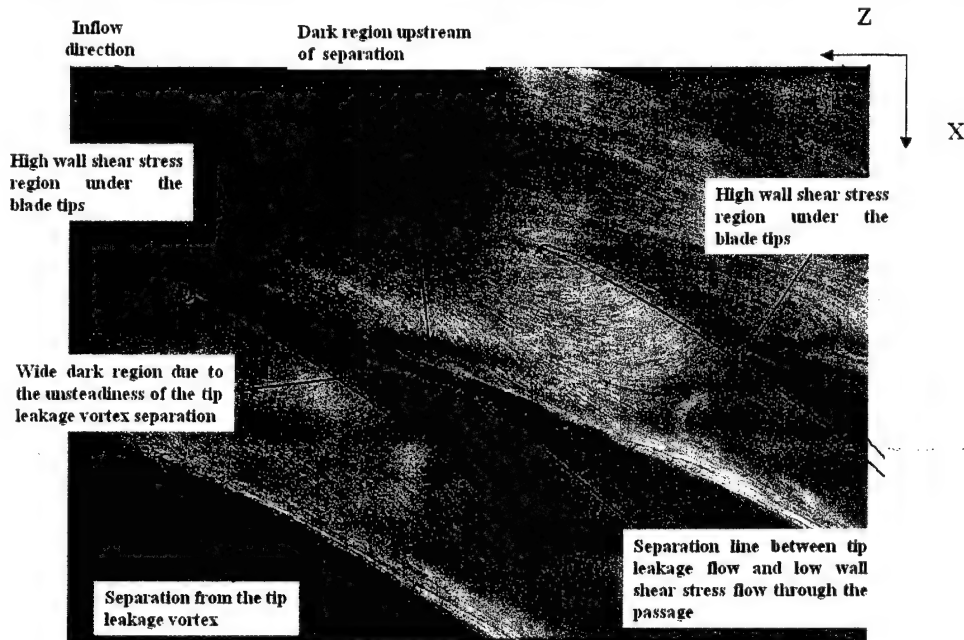Figure 3. Oil flow visualization on the end-wall in the bed coordinates   (Muthanna, 2002, t/c=1.65%)

Figure 4. Oil flow visualization on the end-wall in the bed coordinates   (t/c=3.3%)

this line and x-axis in the bed coordinates is measured as the oil flow angle from the oil flow image, choosing the counter clockwise as the positive direction. In order to get the best tangent line, the streaks are magnified at least 20 times and then the tangent line is drawn. The uncertainty for the direction of the tangent line, which is based on several independent angle measurements on the same streak, is less than 2 degrees, at 20:1 odds. Those streaks in the oil flow pictures correspond to the local oil

flow direction, which can be measured and compared with the average flow angle in the viscous sublayer from the LDA measurements at the same position.

3 RESULTS AND DISCUSSION
3.1 CASCADE FLOW FEATURES BASED ON OIL FLOW VISUALIZATIONS

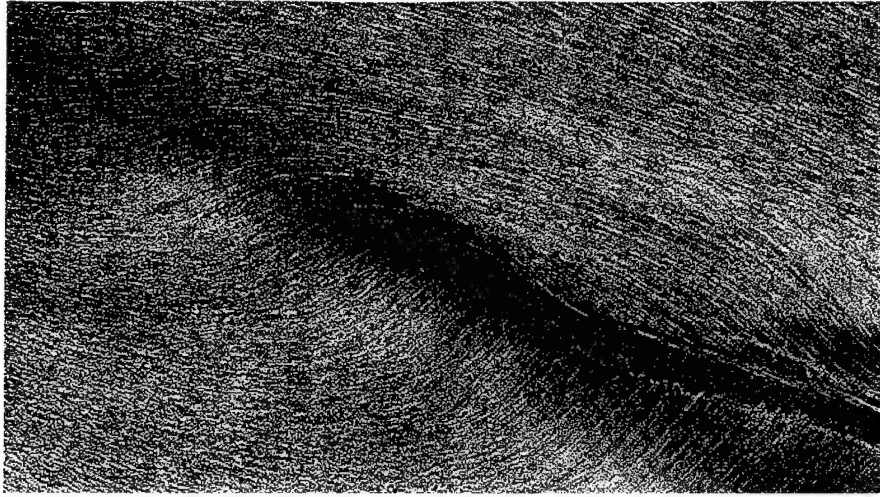From the details of the flow patterns in figures 3 and 4

4

Figure 5. Wall shear stress direction measurement using digitized oil flow picture

that are extracted from the oil flow images, there are two different flow regions in the cascade end wall flows. One is the flow along the passage between the blades, and the other one is the cross flow under the tip gap, driven by the pressure difference between the pressure and suction sides of the blade. These two different flows meet together on the suction side of the blade and roll up, forming the tip leakage vortex. Assuming that the dark regions in the flow visualization that sweep away the oil flow mixture correspond to regions of high shear flow, we observe two dark regions from the details of the flow visualization in each oil-flow image. One dark region is underneath the blade, mainly in the middle part of tip gap region, as shown in figures 3 and 4. This high shear flow is responsible for removing the white titanium dioxide pigment and leaving the dark streaks, as a result of this pressure driven cross flow. These streaks are almost perpendicular to the blade chord. A second dark region is next to the tip leakage vortex cross flow separation region, as shown in figures 3 and 4. This region is where the flow lifts off of the wall. Since a cross flow separation region has locally low friction magnitude (Wetzel et al, 1998), the width of the dark region around the separation line is probably due to the low frequency unsteadiness of the tip leakage vortex.

3.2 GOVERNING EQUATIONS IN THE OIL FLOW SHEET

The oil flow visualization technique enables one to investigate quickly and easily the nature of the flow over the end wall in the linear cascade tunnel. The oil sheet is painted with a prepared paint consisting of a finely powdered titanium dioxide, kerosene, and acid. While the air blows over the oil surface and drags the oil with it, the streaky deposit of the titanium powder remains to mark the local oil flow direction of the flow at the oil sheet surface. The gravitational and pressure gradient effects may cause the oil streaks to be misaligned with the local flow direction at the surface. In the cascade tunnel, a tremendous pressure gradient exists under the blades and on the suction side of the blade (Tian, 2003). The relationship between the local oil flow direction and the wall shear stress direction needs to be reviewed.

The motion of a thin oil sheet on a surface under a turbulent boundary layer was examined by Squires (1962). The following equations governing the motion of a thin oil sheet under a turbulent boundary are given as equations (1) and (2) without gravitational effects

$$U = \frac{1}{\mu}\left[\frac{\partial P}{\partial x}\left(\frac{y^2}{2} - hy\right) + \tau_x y\right] \qquad (1)$$

$$\dot{W} = \frac{1}{\mu}\left[\frac{\partial P}{\partial z}\left(\frac{y^2}{2} - hy\right) + \tau_z y\right] \qquad (2)$$

Here τ_x and τ_z are the x and z components of the mean skin friction in the turbulent boundary in the bed coordinates, which can be calculated by using the least square fit to the viscous sublayer velocity data from the LDA measurements (Tian, 2003). Also U and W are the

5

mean velocity components of the oil flow at the position y; μ is the viscosity of the oil; $\frac{\partial P}{\partial x}$ and $\frac{\partial P}{\partial z}$ are the static pressure gradient components on the end wall; and h is the oil thickness. During the process of forming the visualization, the oil thickness becomes thinner as the air drags the oil away, and it is reasonable to assume that y is equal to the oil thickness, and the equation becomes

$$U = \frac{1}{\mu}\left[-\frac{h^2}{2}\frac{\partial P}{\partial x} + \tau_x h\right] \qquad (3)$$

$$W = \frac{1}{\mu}\left[-\frac{h^2}{2}\frac{\partial P}{\partial z} + \tau_z h\right] \qquad (4)$$

In the visualization process, the oil thickness changes from the initial thickness to close to zero. In the cascade flow, the largest pressure gradient is along the z direction, and at most the magnitude of $\frac{\partial P}{\partial z}$ is about 700 times the τ_z. The oil thickness is about $0.0001m$. While $h \to 0.0001m$, $-\frac{h^2}{2}\frac{\partial P}{\partial x}$ and $-\frac{h^2}{2}\frac{\partial P}{\partial z}$ approach zero much faster than $\tau_x h$ and $\tau_z h$, and equation 3 and 4 become,

$$U = \frac{1}{\mu}(\tau_x h) \qquad h \to 0.0001m \qquad (5)$$

$$W = \frac{1}{\mu}(\tau_z h) \qquad h \to 0.0001m \qquad (6)$$

Considering $\tau_x = \tau\cos(\theta_1)$ and $\tau_z = \tau\sin(\theta_1)$,

$$\tan(\theta_2) = \tan(\theta_1) \qquad (7)$$

Where θ_2 is the oil flow direction and θ_1 is the wall shear stress direction.

It theoretically proves that as the oil thickness becomes thinner and thinner, the oil flow direction is more aligned with the wall shear stress direction, except near separation, where oil material accumulates and h is not zero.

3.3 COMPARISON OF OIL FLOW VISUALIZATIONS AND LDV RESULTS

The governing equations in the motion of the oil flow sheet reveal that the oil flow direction is independent of the viscosity of the oil and becomes less dependent on the pressure gradient as the oil thickness becomes thinner. In the real oil flow visualization experiment, the initial oil thickness depends on how the oil is painted on the oil sheet, which depends on the oil mixture, different brushes, and different strokes. During the process of the visualization, the upstream oil thickness becomes thinner as the air blows the oil to regions of lower skin friction. Close to the separation line of the tip leakage vortex, oil accumulates and the oil thickness is much higher than other places, $-\frac{h^2}{2}\frac{\partial P}{\partial x}$ and $-\frac{h^2}{2}\frac{\partial P}{\partial z}$ are no longer negligible, and the oil flow direction is not closely in the wall shear stress direction.

The oil flow angles measured from the oil flow images match well with wall shear stress angles from the LDA velocity data in figure 6, except those regions close to the tip leakage vortex separation line, which produce large angle differences. Here, wall shear stress direction is defined as the average flow angles from the LDA measurements in the viscous sublayer ($y < 0.0001m$). The root mean square of the flow angle differences, except locations close to the separation line, is $\pm 1.65°$. The uncertainty of the flow angles from the LDV measurements is approximately $\pm 0.5°$ at 20:1 odds (Kuhl, 2001) and the angle uncertainty from the oil flow measurement is about $\pm 2°$. Thus this produces confidence in these wall shear stress angle measurements from the oil flow images away from separation. Oil flow images are a relatively simple way to measure wall shear stress angles for those positions without LDV data.

For each tip tap, in figures 7 and 8, there were more than 1000 wall shear stress angles measured. These angles covered the region between and under blades, including where LDV measurements are available. The near wall passage flow and tip leakage cross flow are captured as shown in these two figures. In figures 9 and 10, in the upstream regions of the passage, the oil flow angles are approximately in the direction of the free-stream at 70 degrees angle to the x-axis in the bed coordinates. While going downstream, the cross flow becomes progressively stronger, the tip leakage vortex forms, and the wall shear stress angles change from the
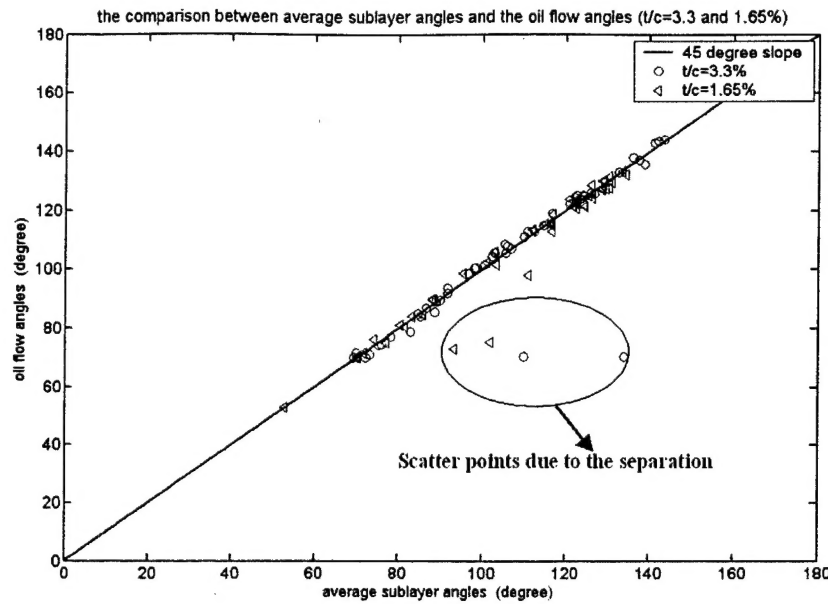
6

the comparison between average sublayer angles and the oil flow angles (t/c=3.3 and 1.65%)

Figure 6. The comparison between the average viscous sublayer flow angles and the wall shear stress angles (t/c=3.3 and 1.65%)

Wall Shear Stress Direction t/c=1.65% (bed coordinates)
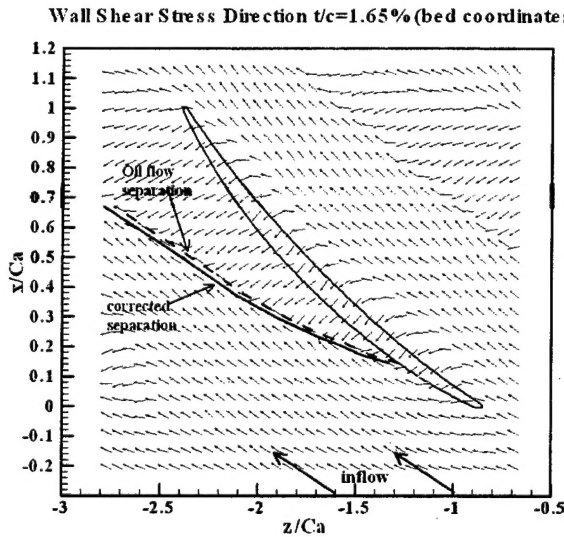

Wall Shear Stress Direction t/c=3.3% (bed coordinates)

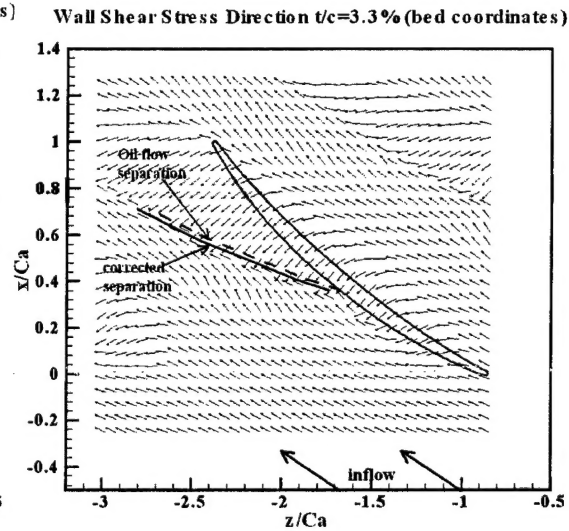Figure 7. Wall shear stress directions t/c=1.65% (measured from the digitized oil flow pictures)

Figure 8. Wall shear stress direction t/c=3.3% (measured from the digitized oil flow pictures)

cross flow direction to the passage flow direction from the pressure side to the suction side of the blade and across the separation.

3.4 THE CALIBRATION OF THE SEPARATION LINE

For a two-dimensional flow, separation or detachment is located where the skin friction is zero. For a three-dimensional flow, a cross flow separation line passes through local minima skin friction locations (Wetzel *et al*, 1998). The mean velocity perpendicular to this separation line is zero, as confirmed by LDA measurements. From the friction velocity calculation with pressure gradient (Tian, 2003), for the t/c=1.65% tip gap, the local minima friction velocity is at z/C_a=-1.455 in the x/C_a=0.18 cross plane and the separation line from the oil flow at the same cross section passes through

7

z/C_a=-1.406. Thus the separation line from the oil flow should move Δz =0.049C_a toward the suction side in order to be more correct, as shown in figure 7. For the t/c=3.3% tip gap, the local minima friction velocity is at z/C_a=-2.04 in the x/C_a=0.42 plane and the separation line from the oil flow at the same cross section is at z/C_a=-1.976. Thus the separation line from the oil flow should move Δz=0.064C_a toward the suction side in order to obtain the more correct, as shown in figure 8. In

both cases, it is assumed that the directions of the oil flow separation line and the corrected separation line are the same. In both cases, the separation line of the oil flow is much closer to the blade than the calibrated separation. Apparently the dominant forces that act on the finite thickness oil flow material around the separation are from the upstream passage flow, which moves the oil-flow separation line downstream of the actual line.
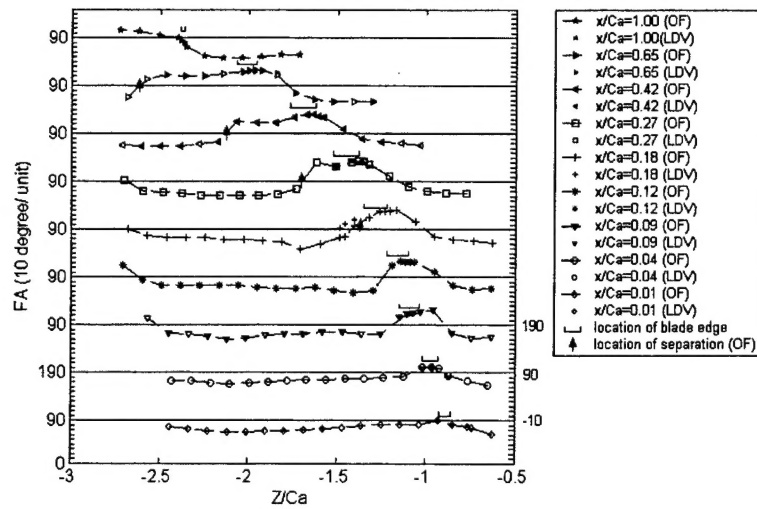

Figure 9. Wall shear stress angles from digitized oil flow pictures for t/c=1.65%
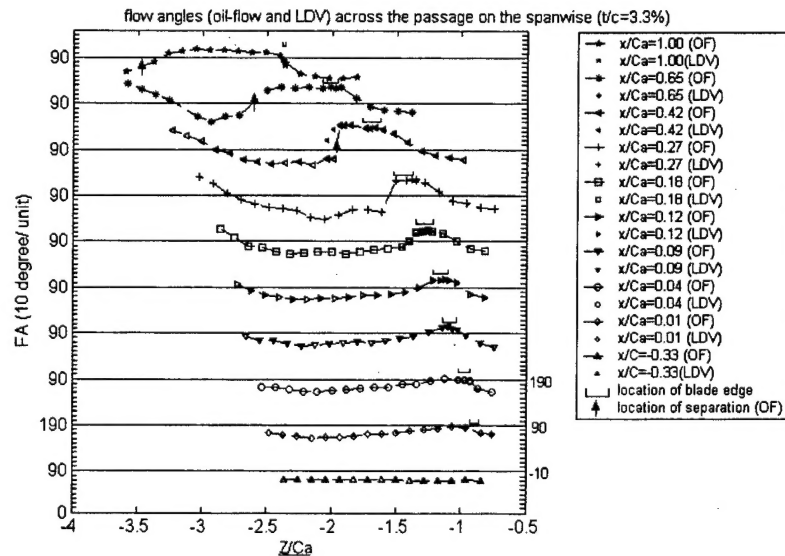

Figure 10. Wall shear stress angles from digitized oil flow pictures for t/c=3.3%

8

4 CONCLUSIONS

Oil flow visualization is a simple and efficient way to capture the time-averaged near wall flow direction features. Motion of the oil mixture driven by the flow and the formation of the oil flow patterns can be clearly obtained and recorded. Theoretically, the oil flow direction is aligned with the wall shear stress direction, where the oil thickness is close to zero. The oil flow streaks are aligned with the direction of the skin friction, without gravitational and boundary layer separation effects, and the effect of the oil flow on the boundary layer motion is very little. The low frequency unsteadiness of the tip leakage vortex may partially contribute to the difference between the oil flow direction and wall shear stress direction close to the separation line. The dominant forces that act on the finite thickness oil flow material around the separation in the cascade flow are from the upstream passage flow, which moves the oil-flow separation line downstream of the actual line.

5 ACKNOWLEDGEMENTS

REFERENCES

Chesnakas, C.J. and Simpson, R.L, 1994 "Full three-dimensional measurements of the corss-flow separation region of a 6:1 prolate sheroid" Experiments in Fluids, vol. 17, pp.68-74.

Kuhl, David Derieg, 2001, "Near Wall Investigation of Three Dimensional Turbulent Boundary Layers" M.S. Thesis, Virginia Polytechnic Institute and State University.

Muthanna, C., Witmer, K. S. and Devenport W.J., 1998, "Turbulence Structure of the Flow Downstream of a Compressor Cascade with Tip Leakage", AIAA 98-0420.

Muthanna, C., 1998, "Flowfield Downstream of a Compressor Cascade with Tip Leakage", M.S. Thesis, Virginia Polytechnic Institute and State University.

Prasad, C.P.K., 1977, "Tip Clearance Effect in Axial Flow Turbines", Indian Institute of Science, Report No. ME-TURBO-1-77.

Squires, L.C., 1962, "The motion of a thin oil sheet under the steady boundary layer on a body", Journal of Fluid Mechanics, Vol. 11, pp.161-179.

Tian, Q., 2003, "Some Features of Tip Gap Flow Fields of a Linear Compressor Cascade", M.S. Thesis, Virginia Polytechnic Institute and State University.

Tang, Genglin, Simpson, R. L., and Tian, Qing, 2004, "Measurement of the tip-gap turbulence structure for a stationary end-wall in a low-speed compressor cascade", Under consideration for publication in AIAA journal.

Wetzel, T. G., Simpson, R. L., and Chesnakas, C. J., 1998, "Measurement of Three-Dimensional Crossflow Separation", AIAA Journal, Vol. 36, No. 4, pp. 557-564.